VKI Lecture Series

# Numerical Investigations in Turbomachinery: A State of the Art

# Large Eddy Simulation Applications

G. Dufour, N. Gourdain, F. Duchaine, O. Vermorel, L.Y.M Gicquel,
J.-F. Boussuge and T. Poinsot

Notes prepared for
the von Karman Institute for Fluid Dynamics
September, 21-25 2009

Contact: gdufour@cerfacs.fr
http://www.cerfacs.fr

# Contents

# Chapter 1

# Introduction

Since Computational Fluid Dynamics (CFD) simulations have become central in the design process of turbomachinery components, the need for as accurate predictions as possible has followed the constant increase in computing power (see Horlock and Denton [57] for an historical review of design practices). Early on and since the pioneering approaches relying on single element/single passage (see Refs. [51, 4] for instance), CFD simulations have evolved to include multiple rows, using the mixing plane approach under the steady flow assumption [30, 28]. With increasing stage loading and reduced weight, strong interactions between rows have fostered the emergence of fully unsteady simulations [100, 47, 53]. Now, state-of-the-art unsteady simulations can be performed on the entire geometry of a multi-stage compressor, including all the passages of all the blades [141, 44]. All the published literature for such applications presents approaches within the (Unsteady) Reynolds-Averaged Navier-Stokes (U)RANS equations framework.

The RANS approach relies on the assumption that turbulent activity can be accounted for using a statistical framework: every flow variable is decomposed into the sum of a (statistical) mean and a fluctuation. The main challenge for RANS modeling is then to model the impact of the higher moments of the fluctuations on the mean flow. However, it is now well recognized that turbulence can play a significant, even dominant, role in the establishment of the mean flow features. In such cases, it becomes of paramount importance that the most energetic turbulent scales are properly accounted for, with as minimum modeling as possible. In this context, Large Eddy Simulation (LES) is a very efficient approach, which allows to model only a part of the turbulence scales, while computing most of the energy-containing scales.

To restrict the scope of this lecture, the choice is made not to deal with what is broadly termed "hybrid RANS–LES" methods. As stressed in recent rewiews (see Sagaut and Deck [113] or Tucker and Lardeau [138]) it is most likely that such approaches will be the first way for "some degree of LES" to be applied to practical engineering applications. However, this is too vast a subject to be included here. Generally speaking, hybrid approaches are divided into: (i) global methods, where only one model is used, ensuring a continuous treatment that blends RANS and LES. The DES method proposed by Spalart *et al.* [131] is the most popular of these methods. (ii) Zonal approaches are the second category, where some kind of two-layer model is used, such as in the ZDES approach of Deck [26] for instance. The interested reader is further referred to the review performed by Batten *et al.* [11] or the results of the DESider European project [46] for instance.

In an industrial context, numerical simulation in turbomachinery is used to predict different

quantities, depending on the intended use of the result [23, 22, 57]: Integrated quantities at inlet and outlet are used to predict overall performances maps (mass flow, pressure ratio, efficiency) to assess the global behavior of a turbomachine. Local flow properties (pressure and velocity distributions) can be used to review design criteria. Steady or unsteady pressure loads are used to assess the mechanical integrity of blades. Wall temperature and heat fluxes are monitored in high-temperature applications. Finally, the unsteady flow field can be used to predict noise [142, 112, 105], usually based on some aeroacoustic analogy.

Depending on the quantity observed, different levels of modeling yield different accuracy: It is generally believed that steady pressure loads can be fairly predicted with a steady RANS approach (even on relatively coarse meshes). Close to the nominal operating point, overall performance of isolated rows (or even multi-stage turbomachines) can be quite well predicted with steady (mixing-plane) RANS simulations. It is thought that unstable operating points (stall or surge) need to resort to URANS approaches. When unsteady pressure loads are sought (for flutter predictions for instance), URANS has proved successfull in predicting the large deterministic (blade-passing-frequency related) interactions in multi-stage turbomachines. On the contrary, when nonequilibrium turbulence plays a significant role in the structuring of the mean flow properties, it is thought that the RANS framework fails to yield satisfactory results. As mentioned in reviews by Lakshminarayna [69] and Bradshaw [17], some of the main challenges faced by the RANS approach in turbomachines are: the prediction of the effects of rotation and curvature, compressibility or pressure gradients, and in particular laminar to turbulent transition. These features, which need to be modeled with *ad hoc* approaches in the RANS framework (see for instance Ref. [35, 129]), are intrinsically captured by the LES approach. However, the LES approach requires significant efforts, among which grid resolution is probably one of the most important in an industrial context.

The objective of the present lecture is to provide an overview of what can be achieved today using state-of-the-art Large Eddy Simulations for turbomachinery components, emphasizing the gain in accuracy and the cost of the method. First, a review of the published literature is performed, highlighting notable achievements in terms of turbomachinery applications with LES. In the second part, two applications of LES in turbomachinery are presented. The first application is a high-pressure turbine stator, the VKI Turmunsflat case, experimentally studied by Sieverding *et al.* [128]. Simulations with the RANS, URANS and LES methods are compared, clearly illustrating the fundamental differences between the three approaches. The computational cost of the methods is assessed, and compared against the benefits in terms of physical accuracy. The second test case is a highly-loaded high-pressure turbine blade cascade studied within a Conjugate Heat Transfer (CHT) framework. This multi-physics case illustrates the coupling between a LES flow solver and a solid heat-transfer code. Comparisons are made to assess the relative gains obtained with the LES approach (as compared to a RANS simulation) and due to the coupling with the heat-transfer code (as compared to adiabatic simulations).

# Chapter 2

# Literature overview of LES applications in turbomachinery

**Contents**



In the last 30 years or so, the LES approach has undergone considerable progress, making it progressively move from a fundamental research tool to a prospective tool [81, 113]. Indeed, LES can now be used to elucidate many complex flows physics [127, 90]. In the past few years, it has demonstrated its capability to handle real-life geometries and flow conditions provided that a substential computational effort is made [107, 64, 13, 48]. Turbulent combustion is an area where this is particularly true [1, 6, 16]. This has showed the potential of LES to be used as an investigation tool with regards to industrial problems. However, LES has still not reached the level of maturity needed to be included in routine design investigations. The first reason for this is linked to computational time issues, because design investigations have to be performed on a daily basis in industry. Furthermore, to reach such a maturity level, many issues need to be addressed, such as wall modeling, numerical schemes, boundary conditions . . . , notwithstanding the need for efficient massively parallel computing architectures and programming techniques. This is especially striking in the turbomachinery field, where few application cases have been performed.

As the present note deals with application cases, the choice is made to structure the discussion from the application standpoint, rather than around technical issues. In this respect, we make the choice to roughly split LES of turbomachinery configurations into three categories:

- **Idealized elementary configurations**, representative of turbomachinery-specific issues. These simulations aim at being reference numerical experiments, unraveling mechanisms previously hidden by other phenomenon and interactions.
- **Basic configurations**, operating at moderate Reynolds numbers, with clearly-defined boundary conditions, usually with weak 3D effects and easy to mesh. The goal of these simulations is to provide insight into previously observed phenomenon, and to deepen our understanding of specific issues. One of the main outcome of such knowledge is its use for RANS turbulence model development (see Refs. [9, 10] for instance).
- **Real-life complex geometries**. Although not completely mature for the design process, such simulations allow the prediction of complex interactions and unsteady effects, so as to give practical engineering information or elucidate complex physics.

Obviously, this classification is somewhat arbitrary, and the separation between each item can be blurry, depending on what specific parameters are used to describe the test case (e.g., geometry, Reynolds, flow features...).

This chapter briefly reviews applications published in the literature for those three categories. Particular attention is given to landmark achievements.

## 2.1 Idealized configurations

Flows in turbomachines are recognized as being very complex, due to important viscous and three-dimensional effects, as well as complex turbulent mechanisms. Pronunced 3D effect are trigerred by streamline curvature, system rotation, relative movement between rows and by clearance gaps. As mentioned in the introduction, the turbulent activity is also subject to complex influences. All these phenomena interact, making it difficult to isolate one among the others. It is therefore of fundamental interest to study simplified configurations, aiming at reproducing some of the salient features of the whole flowfield. The goal is twofold: establish a fundamental understanding of the flow mechanisms and, in certain cases, provide information for RANS modeling.

In this section, several simplified configurations pertaining to the turbomachinery field are first briefly reviewed. Then, particular emphasis is given to work performed on the analysis of the the tip-clearance flow, as it is a configuration very close to that encountered in real-life applications.

### 2.1.1 Channels and ducts

Channel and ducts are the basic component of internal flows, and have been studied extensively with techniques ranging from RANS to Direct Numerical Simulation (DNS). However, there has recently been a renewed interest to study these flow with LES in the perspective of turbomachinery applications, with particular emphasis on cooling applications.

Saha & Acharya [114] studied heat transfer in a rotating duct with ribbs, comparing URANS and LES results. Fair agreement (within 20 % for the heat flux coefficient) with the experiments is observed for both methods. The LES results highlight the role of unsteady coherent structures in the mixing and heat transfer in the duct. Unsteady RANS results do exhibit pronunced unsteadiness in the high rotation regime. Sewall & Tafti [125] study a similar configuration. Their analysis focuses on the detailed flow mechanisms within the duct, and shows the importance of the buoyancy parameter.

Sewall & Tafti [124] also study a stationary 180° bend ribbed cooling duct, analyzing the influence of positionning a rib within the bend.

Elyyvan & Tafti [38] conducted LES simulations of a channel with dimples and protrusions over a range of Reynolds number, ranging from laminar, weakly turbulent to fully turbulent.

### 2.1.2 Enclosed rotor-stator cavities

The simplified geometry of a cavity between a stationnary and a rotating disk has received much attention, both from the experimental and numerical points of views. From the turbomachinery field standpoint, this configuration is relevant to applications such as axial thrust bearings and turbine disk cooling. More fundamentally, it is one of the simplest flow to study 3D effects in turbulent boundary layers.

Several authors have performed DNS of this configuration: Wu & Squires [146] studied a simplified configuration, low rotation rates were studied in Refs. [121, 103], and Lygren and Andersson [80] performed reference simulations for actual cavities. LES predictions were first proposed by Wu & Squires [146]. More recently, Andersson and & Lygren [2] used LES to assess the influence of some geometrical parameters, while Séverac and co-workers [123, 122] performed simulations using a spectral vanishing viscosity technique to study the structure of the three-dimensional turbulent boundary layer.

### 2.1.3 Film cooling

Maintaining wall temperature below certain limits is a key issue in gas turbine design (see section 3.2), which require the extensive use of film cooling techniques. From a fundamental point of view, neglecting the temperature and gradient differences, the basic flow configuration involved is the jet-in-crossflow (see Refs [61] or [99] for instance).

Several studies [68, 54, 1] have shown the limitations of the RANS approach to predict jet-in-crossflow characteristics without *ad hoc* modifications (see Refs. [92, 84] for examples of such modifications). This is mainly due to the strong anisotropy of the Reynolds stress tensor in this configuration, with significant lateral shear stress that impact the mixing and spreading of the jet. This has motivated a number of LES studies of jet-in-crossflow configurations.

Some elementary turbomachinery film-cooling configurations have been studied with LES to study the physics of the flows. Tyagi and Acharya [139] studied the cooling flow from an inclined cylindrical jet using an immersed boundary approach. Very good agreement is found with experimental data concerning time-averaged velocity profiles and film-cooling effectiveness. The LES approach allow the identification of the role of hairpin-shaped vortices in the unsteady heat transfer.

Iourokina and Lele [58] studied the film-cooling flow around a turbine-blade leading-edge configuration. Their approach rely on coupling a low-Mach-number code in the plenum and cooling holes with a compressible code for the leading-edge flow. Particular emphasis is put on the evaluation of the coupling strategy. The analysis of the vorticity dynamics sheds some light on the details of the flow structure.

Finally, Rozati and Tafti [111] studied an idealized cylindrical leading-edge configuration at a Reynolds number of 100,000 based on the cylinder diameter and free stream velocity. An hybrid structured/unstructured grid is used, with a total of 3,211,264 cells. Coherent structures are analyzed, including counter-rotating vortex pair and hairpin vortices. Quantitative and qualitative influence of the blowing ratio is finally discussed and found in good agreement with experimental data.

### 2.1.4 Tip clearance

The gap between a rotating blade tip and the shroud is termed "tip clearance" and is responsible for many important phenomena in turbomachines. Its basic effect is to influence the formation of secondary flows, significantly contributing to the formation of the jet/wake pattern in centrifugal compressors for instance, with a strong influence on efficiency. In transonic compressors, its interaction with the passage shock can be the main factor to trigger surge. For liquid-handling pumps, the tip-clearance flow, and in particular the turbulence generated by the tip-leakage vortex, can induce cavitation because of low-pressure fluctuations.

In this context, a thorough and extensive study of a simplified configuration of tip-clearance flow has been performed at Stanford University by You and co-workers [147, 149, 148, 150] using LES. The configuration is a blade of constant section, with a moving casing, operated at a Reynolds number of $4 \times 10^5$. Experimental studies for such a simplified configuration exist [93, 94], providing a basis for the validation of numerical simulations. However, there is a need for detailed information regarding the turbulence properties and the unsteady nature of the flow, which can still not be measured. Given the large range of length and time scales involved by this flow, the RANS approach is not well suited, and LES has been deemed the most appropriate tool.

From the practical point of view, a first important constraint for the studies performed by You and co-workers is the grid density. In early work [147], a grid with "only" 7.9 million points proved insufficient: too coarse a streamwise resolution delayed the formation of the tip-leakage vortex and caused its early breakdown. Use of a 20 million points mesh improved the predictions [149]. It allowed the analysis of the tip-leakage vortex formation, trajectory and breakdown: they appear to be linked with the prediction of the separation area on the blade suction side. This is illustrated in Fig. 2.1-(a).

Specific challenges with respect to the numerical approach for this flow are synthesized in Ref. [148]. Concerning the mesh generation process, an immersed boundary method was developed, which allowed to increase the quality of the mesh while reducing grid density. As previously mentioned, the mesh density is essential, but also is its quality. As observed in previous studies [89], the divergence and skew-symmetric forms are to be preferred when dealing with skewed meshes, as is often the case in complex geometries when structured meshes are used. The final grid [150] consists of $449 \times 351 \times 161$ points in the streamwise, tangential and spanwise directions, respectively. In particular, at least 30 mesh points are clustered in the tip-gap. A point of concern is the generation of inflow turbulent conditions: the method of Lund [79] is used, with a modification to account for the flow direction.

The detailed mechanisms of the turbulence generation process and end-wall vortex dynamics were further analyzed [150], with a perspective on the influence of the tip gap size. As could be expected, the turbulent kinetic energy is generated in zones of high vorticity, created by the gradients associated to the tip-leakage vortex and jet [see Fig. 2.1-(b)]. It is further found that this mechanism holds regardless of the gap size: this is an important conclusion, which suggests that a methodology for design considerations can be developed for all gap sizes. On the other hand, the formation and the trajectory of the tip-leakage vortex are modified as the tip-gap size changes: the vortex forms further downstream as the tip-gap size increases and becomes more inclined with respect to the blade chord. This understanding of the flow feature provides a sound basis for further development of active or passive control strategies [42].

A similar configuration has been addressed by Boudet *et al.* [15], with the perspective to study aeroacoustics effects.

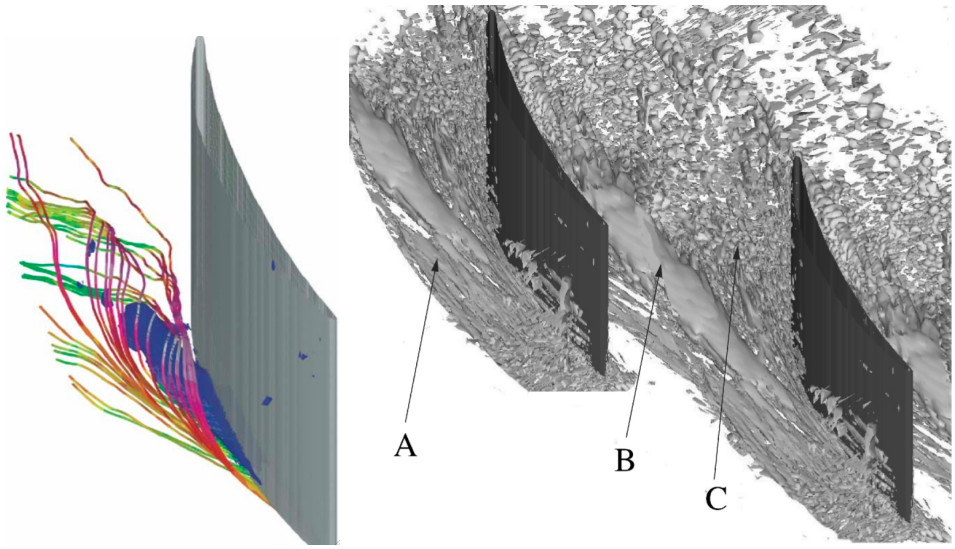


(a) Isosurfaces of pressure with stream traces

(b) Isosurfaces of $\lambda_2$ criteria showing vortical regions

Figure 2.1: LES of a simplified tip-clearance flow. The tip clearance is located at the bottom of the blade. Results from You *et al.* [148, 150]

## 2.2 Basic configurations

This section deals with configurations that are representative of the turbomachinery field, but somewhat basic or idealized in some way.

### 2.2.1 Low pressure turbine

Although most real-life turbomachinery components operate at high Reynolds numbers (around the million), there is the specific case of low-pressure turbines. Placed after the high-pressure turbine, the fluid entering the low-pressure stage has a low density, and therefore a low Reynolds number. This specificity makes the LES approach more affordable, because of lower mesh constraints. Although the real fully 3D geometry of industrial turbines is not simulated here, the idea is to deal with representative blade sections and flow conditions.

A case that has received much attention is the T106 low-pressure blade, which was experimentally studied under different flow conditions [55, 132, 96, 97]. The LES results discussed in the present section deal with two phenomena: the unsteady behavior of a laminar separation bubble and the effect of incoming wakes, which are both highly dependent on the turbulent fluctuations.

#### Laminar separation bubble

Raverdy *et al.* [104] have simulated the unsteady behavior of a laminar separation bubble over the T106 blade at a Reynolds number $1.1 \times 10^5$ based on the inlet velocity and the chord, with an inlet Mach number of 0.1. The configuration studied is based on the experiments performed by Hodson [55]. This test case is particularly suited to assess the benefit of LES because of its transitional nature, which conditions the length of the bubble. Furthermore, the phenomenon is highly unsteady, with a spectrum covering a large range of frequencies.

The LES methodology set up by Raverdy and co-workers relies on the MILES approach [14, 32], that is to say no subgrid scale model is used and the convection scheme is assumed to

cascade the energy down from the resolved to the subgrid scales. To this end, the AUSM + (P) [83] upwind scheme is used. Implicit time integration is performed. Mesh convergence is assessed by using several grid resolution, and seems to be reached thanks to a local mesh refinement technique, where spanwise discretization is reduced in laminar areas. Bridging of the zones with different spanwise resolutions is performed with first-order extrapolation.

After performing a successfull validation of both the mean and fluctuating quantities, the authors proceed to analyze the formation of the laminar separation bubble. The route to turbulence is shown to begin with the roll-up of the separated shear layer under the Kelvin-Helmholtz instability, leading to the ejection of coherent structures, as illustrated in Fig. 2.2

Further unsteady effects are observed, in the form of sustained fluctuations within the recirculation area. Spectral analysis shows that the low-frequency part of the fluctuations locks to that of the vortex shedding at the trailing edge. As will also be illustrated later in the present note, acoustic waves are emitted near the trailing edge, which are responsible for this coupling. They travel upstream to the stagnation point, where they are "reflected" as vortical perturbations which will in turn be convected to the recirculation bubble.

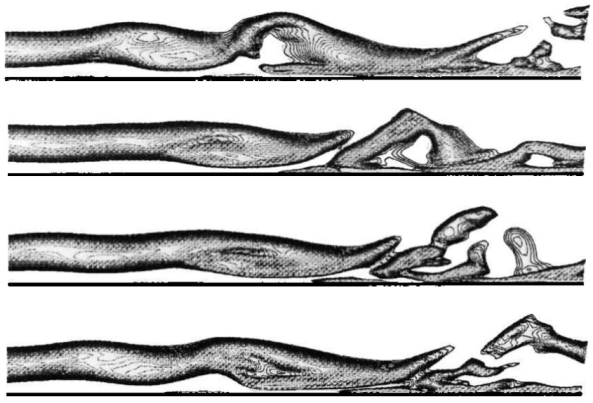

Figure 2.2: LES of a low-pressure turbine. Instantaneous spanwise vorticity near the bubble. Results from Raverdy *et al.* [104].

### Incoming wake

The T106 blade has also been investigated with periodically passing wakes at the inlet. DNS of this case was performed by Wu & Durbin [145]. Michelassi *et al.* [88] have studied this case for a Reynolds number of $1.48 \times 10^5$, based on the inlet velocity and the chord. The main objective of the study is to assess the LES approach as an alternative to DNS for providing reference results to use for RANS model development.

The LES methodology set up by Michelassi and co-workers deals with incompressible flow. Space discretization is performed with a second-order cell-centered finite volume approach. Explicit time marching is performed with a three-stage Runge-Kutta algorithm. Subgrid scale modeling is ensured by the dynamic model (see Germano *et al.* [40] and Lilly [76]). Inflow boundary conditions are the same as those used in the DNS of Wu & Durbin [145], and are generated by a separate LES calculation.

The LES results are shown to provide a good overall picture of the flow. Although transition on the suction side is reproduced, it appears to be delayed by about 10 % of the chord as compared to DNS, probably due to a lack of mesh resolution to capture the interaction of the incoming wakes and the boundary layer. The fluctuating flow field is better reproduced, showing a mildly turbulent regime, where strong favorable pressure gradients inhibits the spanwise and

normal turbulent stresses. An interesting finding is the illustration of how the incoming wakes are responsible for the periodic appearance of turbulent and becalmed region (the so-called "calming" effect [25]).

Similar simulations of the T106 blade have also been performed by Sarkar [117, 115, 116] at Reynolds numbers of $1.6 \times 10^5$ and $7.8 \times 10^4$.

### 2.2.2 Compressor and turbine

Eastwood and co-workers [37] present results obtained on "idealized" compressor and turbine configurations. They study endwall flows on 2.5 D geometries using "Numerical" LES (*i.e.*, without SGS model), and make comparisons with an hybrid RANS/LES approach (the RANS layer is close to the endwall).

The compressor test case has a Reynolds number of $2.3 \times 10^5$ with a Mach number of 0.07 (based on chord and inflow velocity). A 5 million-cell mesh is used. Figure 2.3 shows instantaneous contours of the $\lambda_2$ coefficient (see Ref. [60]), indicating coherent structures over the compressor blade and endwall. Results show fair agreement with the experimental data for the exit flow angle and loss coefficient. Streamlines on the compressor endwall indicate that LES predict separation too far upstream from the leading edge, apparently from insufficient turbulent activity to overcome the adverse pressure gradient.

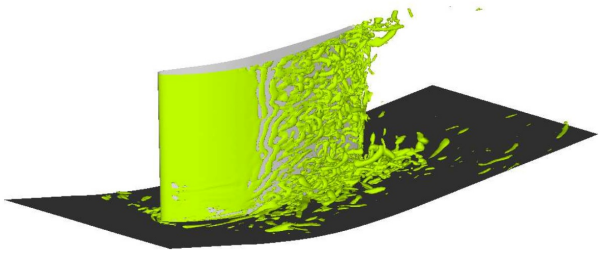

Figure 2.3: LES of an idealized compressor. Instantaneous spanwise vorticity near the walls. Results from Eastwood *et al.* [37].

The turbine test case has a Reynolds number of $5.9 \times 10^5$ (based on chord and inflow velocity). A 5.4 million-cell mesh is used. Modest agreement with the experimental results is observed, partly due to a bad prediction of laminar regions.

For both test cases, improvement were obtained using an hybrid RANS/LES strategy. Given the mesh resolution (as compared to the meshes used by You *et al.* [150]), it is much likely that the mesh density close to the wall was not sufficient for the LES requirements, which explains the improvement with the RANS layer.

Lee *et al.* [72] studied a compressor cascade, using a deductive dynamic SGS model, with mesh resolutions up to $271 \times 124$ in the blade-to-blade plane, and up to 24 points in the spanwise direction. Several blade passages were modeled (up to 4), allowing the study of pitchwise variations from one blade to the other. Studying shedding patterns for various incidence angles (from $-20°$ to $+20°$), they also apply a Ffwocs Williams & Hawkings (FW-H) aeroacoustic analogy to compute the far field noise.

With the 4-blade domain, a pattern of rotating instability was observed. It is linked to the formation of an unsteady vortex due to separation at the leading edge, and the associated

blocking effect, as discussed by Gourdain *et al.* [43] for instance. Comparisons for the pressure loss coefficient against experimental data show a good agreement.

Tauveron [136] studied a compressor cascade in the stalled flow regime, with angle of attacks ranging from 30° to 60°. To the authors knowledge, it is the only published turbomachinery LES study on unstructured meshes. A second-order scheme is used for convective fluxes, and time marching is performed with a second-order Crank-Nicholson scheme. Importance is given to assessing the wall modeling strategy, and standard wall functions [45] are compared against the TBLE formulation [7].

Regarding the pressure loss coefficient, 2D RANS is more accurate than "2D LES". A 3D LES with a sufficient spanwise extend improves the results to about the same accuracy as the RANS. Interestingly, the RANS underpredicts the loss whereas the LES overpredicts it. Slightly better results are obtained with the TBLE approach.

Finally, Tyagi & Acharya [140] studied a simplified turbine stage configuration (stator and rotor). The geometry is assumed to be 2D, and modeled with a spanwise extension of 0.1 blade chord. The flow conditions are set so that the Reynolds number is 5000. A $302 \times 202 \times 11$ point mesh is used. The LES strategy relies on the immersed-boundary method for moving geometries, which relieves much of the burden associated to conservativity issues with sliding mesh techniques. Altghough it is a prospective case, this is one of the few rotor–stator LES calculation published.

This mainly demonstrative calculation is used to analyze the vortices formed in the passage. Vorticity shed from separated area over the stator is shown to interact with the downstream rotor, and convected within the passage.

## 2.3 Complex geometries

### 2.3.1 Pumps

A centrifugal pump impeller has been simulated by Byskov *et al.* [20] at design and off-design conditions. The Reynolds number based on exit diameter and blade circumferential exit velocity is $1.4 \times 10^6$. However, as noted by the authors, basing the Reynolds number on local velocity and blade height yields a significantly lower value of $1.5 \times 10^4$. Two blade passages are meshed with 385 000 cells. The standard Jameson scheme discretizes the convective fluxes, and time-integration is performed with a fourth-order Runge-Kutta scheme. The period is discretized with 160 time steps, and 12 revolutions are found sufficient to obtain converged statistics.

The LES results are compared to steady RANS computations (with the Baldwin-Lomax and the Chien models) and with PIV measurements. At the design point, significantly better agreement with the experiments is found for the LES results. At part-flow conditions, the agreement with the experimental data is much less satisfactory, and only some qualitative features of the LES results seem more accurate than that of the RANS simulations.

A mixed-flow pump was studied by Kato *et al.* [63] using a finite-element method applied on overset grids from dual frames of reference. The pump stage is composed of a four-blade impeller with an eight-blade diffuser downstream within a scroll-like casing. The Reynolds number based on exit diameter and blade circumferential exit velocity is $5.7 \times 10^6$. The mesh is composed

of 5 millions of elements, covering the full 360° of the geometry. The unsteady simulation is performed over 10 revolutions of the impeller.

In the low-flow unstable regime, computed total pump heads are found in fair agreement with the experimentally measured characteristics, although stall is predicted at a 6 % lower flow rate. Predicted phase-averaged profiles of meridional and tangential velocities are found in fair agreement with LDV measurements.

Kato and his-coworkers further worked on a 5-stage centrifugal pump [62, 64], and studied noise generation mechanisms using Lighthill's acoustic analogy.

It should be emphasized that these are, to the best authors' knowledge, the only published cases of LES on **fully** 3D rotor–stator or multistage configurations[1].

### 2.3.2 Axial Fan

Lee *et al.* [72] also studied an axial fan configuration, for which experimental data from the DLR are available [78]. The Reynolds number based on exit diameter and blade circumferential exit velocity is $1.1 \times 10^6$ (see the remark in the previous section on this value). A mesh with 385 000 points is used, consisting of $107 \times 81 \times 47$ points is the streamwise, azimuthal and spanwise directions, respectively. The farfield noise is computed using the FW-H aeroacoustic analogy.

The numerical results show the tip vortex influence on the efficiency and the noise level. Farfield dipole noise as well as unsteady drag and lift forces are found in good agreement with the experimental data.

Studies have been performed at the Onera to predict the broadband noise emitted by an axial fan stage, using aeroacoustic analogy to compute source terms from LES results [108, 105, 106]. They consider a DLR low-speed fan stage (rotor and stator), operating at a Mach number 0.22 and a Reynolds number of $2.2 \times 10^5$. A thin slice of the 3D geometry is computed, with a spanwise extent of about the boundary layer thickness at the outlet of the stator. A reduced number of blades approach is used [3], so that periodic boundaries can be used and only one blade passage for each row is modeled.

The 2.5D grid consists of about 6.3 and 5.9 millions of points for the rotor and stator, respectively. In particular, the O-type blocks around the blades are made of $653 \times 61 \times 37$ points for the rotor, and $605 \times 61 \times 37$ points for the stator, in the streamwise, tangential and spanwise directions, respectively. Including the other blocks, 279 points discretize the pitchwise direction. In terms of wall units, the mesh spacings at the walls are such that $\Delta y^+ \leq 2$ on most parts of the airfoil, $\Delta x^+ \leq 40$ an $\Delta z^+ \leq 20$ all around the profiles.

The Jameson scheme discretizes the convective fluxes, and time-integration is performed with a Gear scheme, using an approximate Newton method to solve the non-linear problem. At each physical iteration, the implicit Gauss-Seidel method is used. SGS modeling is ensured by the WALE approach [95]. In-duct noise field is computed from the LES data using FW-H equations, and radiation is achieved using a Kirchhoff integral approach.

Validation is performed considering the noise levels. In-duct sound power level are found in good agreement with the experiments except in the low-frequency range. Free-field radiation obtained with the Kirchhoff integral is compared to exact solutions obtained with the Wiener-Hopf method: similar sound pressure levels and directivity lobes are obtained, with a significant CPU time reduction for the Kirchhoff method.

[1] Note that Refs. [140] and [108, 105, 106] compute only a slice of a 3D configuration, that is to say their computational domain only covers a small part of the full span of the real geometry.

### 2.3.3 Turbine inlet guide vanes

Black *et al.* [12] studied a cooled inlet-guide-vane configuration for high fuel-air ratios. A 5 million-point mesh is used (including the grid inside the cooling passage and the holes). Reactions are modeled using a two-step kinetics and two-variable assumed probability density function for turbulence chemistry interaction. LES results are compared with $k$–$\omega$ RANS calculations. Turbulent inlet boundary conditions are generated from a separate LES combustor computation, using the procedure of Klein *et al.* [65] to set velocity fluctuations. Time-averaged data are used for the RANS simulation.

The main advantage of the LES approach in this configuration is to take into account the fluctuations at the inlet. In this case, such fluctuations result in fuel-rich pockets which react with the cooling jets, thereby yielding unsteady heat release, as illustrated in figure 2.4, where a snapshot of the temperature field around the blade is shown. Averaged RANS simulation obviously fail to predict this phenomenon. This case clearly highlights the potential benefit of the LES approach, as hot-spot formation can be a major design constraint during turbine conception.

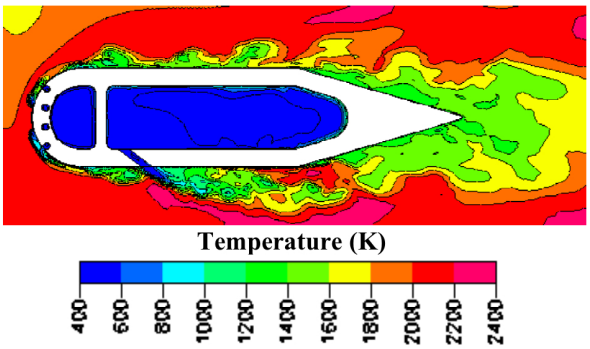


Figure 2.4: LES of inlet guide vanes with cooling. Instantaneous temperature field around the blade. Results from Black *et al.* [12].

### 2.3.4 Axial Compressor

One of the most recent achievement in the LES simulation of complex turbomachinery configuration is the work of Hah [49, 48, 50]. Of particular interest is Ref. [48], where LES is used to elucidate some of the mostly debated flow features occurring in the NASA transonic compressor Rotor 37. The grid used consists of $560 \times 198 \times 124$ points is the streamwise, azimuthal and spanwise directions, respectively, which amounts to about 14 millions of points. The governing equations are solved with a pressure-based implicit method using a fully-conservative approach. A third-order accurate interpolation scheme is used for the discretization of convective terms, which is of second-order accuracy on smoothly varying grids. An implicit second-order scheme with dual-time stepping is used for time integration. The dynamic model of Germano *et al.* [40] is used for the SGS model. RANS results are also given to assess the benefit of the LES approach. The primary goal of the simulation is to elucidate discrepancy often found between RANS results and the experimental data for the Rotor 37, in particular concerning the azimuthally-averaged total pressure and temperature distributions at the rotor exit.

The agreement of the LES results with the experimental data is fairly good, slightly better than the RANS results for the outlet profiles. More importantly, it confirms the presence of a hub corner stall, previously debated among researchers. Better agreement in particular is observed close to the casing, where the results indicate the importance of a self-induced unsteadiness due

to shock/tip leakage/vortex shedding interactions, which is not captured by the RANS approach.

Concerning the overall massflow–efficiency characteristic, significantly better agreement with the experiments is observed for the LES. In particular, near stall, the LES prediction is 1 efficiency point closer to the experimental results than the RANS method.

### 2.3.5 DNS of a Turbine Stage

A special mention is made here of work performed by Rai [101, 102] on the Direct Numerical Simulation (DNS) of the flow in a low-speed axial-turbine stage. The computations rely on a high-order accurate upwind-based, iterative implicit, finite-difference method. A reduced number of blades approach is used [3], so that periodic boundaries can be used and only one blade passage for each row is modeled. The geometry is only "quasi-3D" in the sense that the blades are not twisted. The grid is claimed to be optimized, using adequate DNS resolution only where the flow is expected to be turbulent, but somehow disappointingly, no quantitative information on the mesh resolution is given. Time-averaged and phase-averaged results are compared with the experiments and found in mostly good agreement. An illustrative results is shown on Fig. 2.5, showing the wake on the stator impacting the rotor leading edge, as well as the trace of the previous passing wake in the channel.

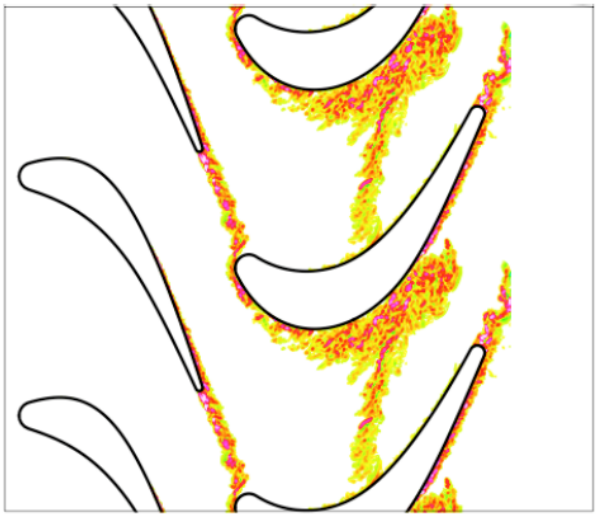

Figure 2.5: LES of a low-speed turbine stage. Instantaneous spanwise velocity. Results from Rai [102].

## 2.4 Synthesis

As mentioned in the introduction, the possible gains of using an LES approach depend on what quantity or phenomenon is examined, while the cost is measured against a (U)RANS approach.

For the channel flow test case presented by Saha & Acharya [114], the goal is to predict heat transfer at the wall. In this case, both URANS and LES methods yield roughly similar accuracy of the overall flux (measured by the absolute distance to the experimental value). However, the flow fields predicted are qualitatively different, with unsteady structures damped in the URANS case, yielding a lower value of the heat flux. The cost of the LES approach (on a mesh with roughly $2^3$ more points) is a factor 6 in computational time compared to the URANS approach.

For the LP Turbine blade simulated by Raverdy *et al.* [104], the goal is to predict the laminar bubble, with obvious impact on the blade aerodynamic characteristics. The prediction

of laminar separation is a challenge for RANS models, and requires *ad hoc* modeling (see Refs. [8, 144, 135] for instance, and Lardeau and Leschziner [71] in particular for the case of wake-induced transition), which is generally not well suited to an industrial context. On the contrary, the LES approach is shown to predict this phenomenon accurately. However, to cope with the important associated grid requirement, the local refinement technique proposed by Raverdy and co-workers seem to require some *a priori* knowledge of the flow.

Considering the idealized compressor and turbine calculations of Eastwood *et al.* [37], it appears that performing a LES to predict outlet flow profiles (total pressure and temperature), as well as flow patterns, on a relatively coarse mesh yields results less accurate than with an hybrid RANS–LES approach. More generally, this raises the question as to wether a "good" URANS calculation can yield better results than a "bad" LES, where good and bad can be related to the grid density (with different requirements for RANS and LES) or boundary conditions (which need to be more sophisticated — in terms of turbulent fluctuations – for LES than for RANS, for instance.

Going to a more practical application, the results of Black *et al.* [12], where the wall heat flux and temperature over a turbine guide vane downstream a combustor chamber are examined, clearly illustrate a sizeable benefit in terms of accuracy for the LES. Indeed, it shows how the inclusion of turbulent inlet fluctuations in the LES, which is of course not possible in the RANS framework, can dramatically alter the results. It is however regrettable that no information is given as to the relative costs of the computations.

# Chapter 3

# Case studies

**Contents**



This chapter presents LES results recently obtained at CERFACS in the field of turbomachinery. The first application is the high-pressure turbine stator of the VKI Turmunsflat case. Comparisons of results with the RANS, URANS and LES methods are presented. The second test case is a highly-loaded high-pressure turbine blade, from the T120 cascade of the AITEB (Aerothermal Investigations on Turbine Endwalls and Blades) European project, studied within a conjugate heat transfer framework. Results obtained with adiabatic RANS and LES approaches are first compared, then the inclusion of heat transfer within the solid is assessed.

## 3.1 High-pressure turbine stator

### 3.1.1 Motivation and problem description

Vortex shedding (von Karman vortices) is known to occur at the trailing edge of turbomachinery blades. This phenomenon, intrinsically unsteady, is important in several respects: (i) it influences the trailing edge base pressure, which in turn conditions the blade profile loss [29]; (ii) the vortices can interact with the downstream rows and produce tonal noise; and (iii) the unsteady pressure loads can affect the structural integrity of the blades. The accurate prediction of the shedding frequency depends on the numerical approach [130] but also on the turbulence modeling [137, 39]. In particular, Manna [82] suggests that correctly predicting the near and far wake requires proper account of the anisotropy, curvature and rotation effects on the turbulence field.

The stator of a high-pressure turbine has been chosen to assess the capacity of LES to correctly predict the vortex shedding occuring at the blade trailing edge. This configuration has been experimentally studied at the VKI by Sieverding *et al.* [128]. The Reynolds number based on chord is $2.8 \times 10^6$, which corresponds to a high value for LES, especially in the light of the cases presented in chapter 2. Measurements indicated the presence of large coherent structures in the turbine blade wakes (von Karman vortices), which largely affect the pressure distribution

around the trailing edge. The objective is to investigate the capacity of the RANS, URANS and LES methods to reproduce this feature. The RANS and URANS calculations are performed with the two-equation $k$–$\omega$ turbulence model of Wilcox [143]. The LES simulation uses the subgrid model of WALE [95]. The convective fluxes are computed with the AUSM+ scheme proposed by Liou [77] and the time integration is performed with a 4-step Runge Kutta method combined to implicit residual smoothing. The simulations are performed with the *elsA* software [21]. Based on the assumption that the flow is mainly 2D, the computational domain represents 10 % of the experimental blade span. The grid used for the RANS and URANS simulations is composed of 0.795 millions of cells, which corresponds to a rather fine grid by RANS standards. The grid considered for LES is more refined and uses 6.37 millions of cells. For both meshes, the grid clustering at the wall is such that, in average, $\Delta y^+ \simeq 1$.

### 3.1.2 Comparison and analysis of the results

Table 3.1 indicates the cost of the three methods. The cost ratio in terms of computational time between RANS and URANS is 11 and the cost ratio between URANS and LES is 9. This one order of magnitude separation between each method is quite significant. It shows the clear need for massively parallel computing resources when dealing with practical, high Reynolds number, LES configurations. With this comes the issue of the scalability of solvers.

| | RANS | URANS | LES |
|---|---|---|---|
| Number of cells | 795 000 | 795 000 | 6 370 000 |
| Cpu Time (hours) | 21 | 230 | 2000 |

Table 3.1: High-pressure turbine stator: comparison of the computational efforts. For the RANS simulation, the time corresponds to a converged steady state solution. For the URANS and LES, it corresponds to 10 ms of simulation. Results obtained with the *elsA* solver on an SGI Altix platform.

A comparison of the instantaneous flow fields is show in Fig. 3.1, where contours of the density gradient are displayed. The overall picture is in line with the theoretical background of the three methods: unsteady effects are not captured by the RANS approach, whereas the URANS and LES predict vortex shedding; the URANS fails to predict detailed flow features observed in the LES and experiments, as discussed below.

The other major defect of the RANS approach is that it predicts the development of a non-physical shock-wave slightly down the throat [see Fig. 3.1-(a)], between the suction side of the blade and the trailing edge of its neighbor. This is due to a difficulty to correctly estimate the boundary layer thickness.

Regarding the URANS approach, though vortex shedding is clearly captured, it fails to predict the complete structure of the acoustic waves and the turbulence streaks in the boundary layer, which are observed in the LES result. These detailed flow features are averaged (in the statistical or phase sense) by the mean of the turbulent viscosity, with a contribution of the artificial (numerical) dissipation related to grid size.

On the opposite, the LES computation clearly shows acoustic waves periodically emitted at the trailing edge, which travel upstream and are reflected on the suction side of the blade. The interaction of these waves with the boundary layer causes the formation of turbulence streaks, which in turn affect the vortex shedding. This phenomenon is quite similar to that discussed by Raverdy [104].

Quantitative comparison with the experimental data is then performed. Figure 3.2 (a) shows the isentropic Mach number distribution over the blade for the RANS and LES methods, defined

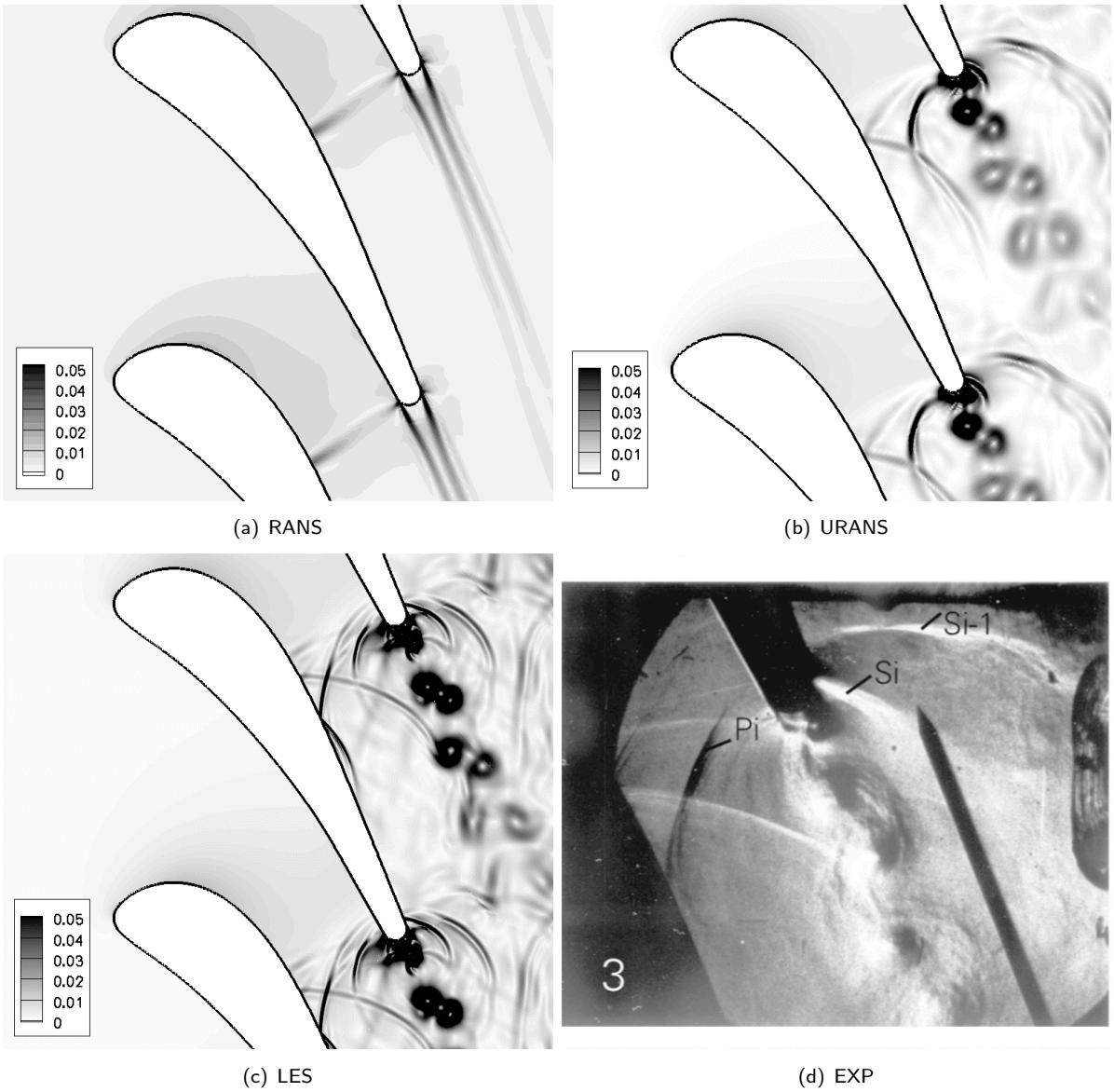


(a) RANS (b) URANS

(c) LES (d) EXP

Figure 3.1: High-pressure turbine stator: comparison of the flow features predicted by the three methods and experimental schlieren from Sieverding *et al.* [128]. Contours of the density gradient.

as:

$$M_{is}(\mathbf{x}) = \sqrt{\frac{2}{\gamma - 1}\left[\left(\frac{P_1^t}{P_w^t(\mathbf{x})}\right)^{\frac{\gamma-1}{\gamma}} - 1\right]}, \tag{3.1}$$

where $\gamma$ is the isentropic coefficient, and $P_1^t$ and $P_w^t(\mathbf{x})$ are the total pressure of the mainstream and at the wall at location $\mathbf{x}$, respectively. As previously mentioned, the RANS simulation predicts a shock-wave on the suction side that is not reported by the experimental work (at a reduced axial position of 0.6). The RANS simulation also under predicts the value of the isentropic Mach number near the blade leading edge on the pressure side. The agreement of the LES results with the experimental data is quite good. The URANS simulation, not shown here, yields very similar results to the LES approach. This is not surprising, as it is well known that pressure distributions are "easy" to predict, provided the main flow features are captured. In the present case, it is unsteady vortex shedding that needs to be accounted for.

The quantitative unsteady features of the URANS and LES results are now discussed. From a global point of view, vortex shedding is characterized by the Strouhal number $S_t = f.D/U$ (where $f$ is the vortex shedding frequency, $D$ the trailing edge diameter and $U$ the external velocity) . The Strouhal number (given in Figure 3.2 (b)) estimated with the URANS method is far from the experimental value (+26 %), while LES gives a correct prediction (+4 %). This is linked to the frequency content of the simulations. Figure 3.2 (b) shows unsteady signals of axial velocity registered at location of 20 % of the blade chord downstream the trailing edge in the wake of the blade. This figure shows that the frequency content of the LES simulation is much richer than that of the URANS simulation. This is due to the fact that the small turbulent structures captured by the LES approach impact the overall flow features (in particular the turbulent streaks previously discussed).

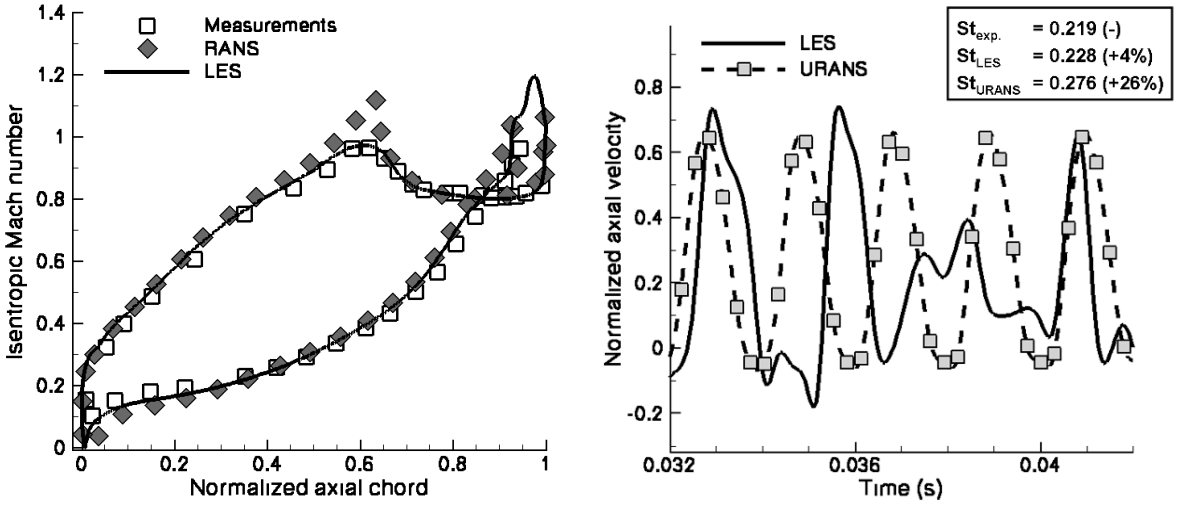


(a) Isentropic Mach number

(b) Unsteady axial velocity signal.

Figure 3.2: High-pressure turbine stator: comparison of the numerical and experimental results.

As a conclusion, this case illustrates the fundamental differences between the RANS, URANS and LES methods with regards to the details of the physics predicted. This is to be balanced with the computing cost, depending on the intended application.

## 3.2 Conjugate heat transfer for a cooled turbine blade

Determination of heat loads is a key issue in gas turbines conception [70, 73, 118, 36, 19], because wall temperatures and heat fluxes are a major constraint in the design of combustor and turbine blades. Indeed, the life duration of turbine components directly depends on the wall temperature and therefore designers imperatively need an accurate prediction tool: a 15 K difference on the temperature at mid-span of a blade corresponds to a reduction of its life duration by a factor 2. Numerical simulations of the thermal interaction between fluid flows and solids is therefore of primary interest. The difficulty is that the complex flows observed in the turbine environment can not be efficiently computed with (U)RANS methods, especially when regarding thermal effects. For example, laminar to turbulent transition, hot spot incoming from the combustion chamber, temperature gradient at walls are among the difficulties that CFD solvers have to address, and much likely better predicted in the LES framework.

The turbulence effect on the heat transfer coefficient $H$ is shown Fig. 3.3 in the Inlet Guide Vane (IGV) of a highly loaded transonic turbine, experimentally studied by Arts *et al.* [5].

This figure highlights the paramount importance of transition on the distribution of the heat transfer over the blade.Today, RANS simulations (even with transition models) performed on this configuration exhibit a very poor predictive capacity and lead to errors higher than 50 % on the value of the heat transfer coefficient. As shown in Fig. 3.3, the difficulty comes from the strong impact of the inlet turbulence level on the transition region (mainly driven by the shock-wave position). In this context, LES emerges as a promising way to increase the reliability of flow solvers.

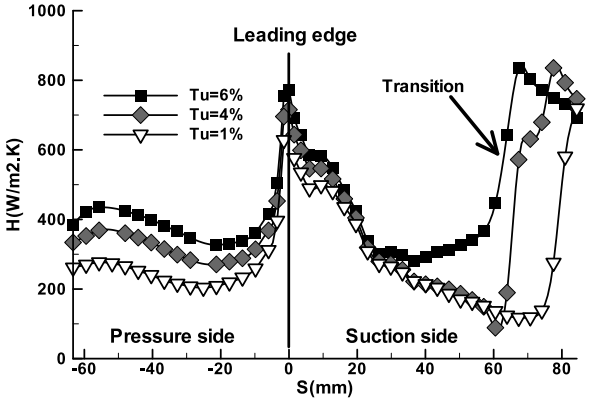


Figure 3.3: Effect of the laminar to turbulent transition on the heat transfer coefficient $H$ (High-pressure turbine stator configuration, experimental results from Arts *et al.* [5].

The study presented in this section, based on work performed by Duchaine *et al.* [34, 33], deals with the coupling strategy of a LES solver and a heat transfer code within solids, applied to the simulation of a cooled turbine blade.

### 3.2.1 Numerical approach and test case

The LES solver used is the AVBP code developped at CERFACS and IFP (Institut Français du Pétrole) [119, 91, 86, 110], which solves the full compressible Navier-Stokes equations on unstructured meshes, using a cell-vertex/finite element approximation and a Taylor-Galerkin weighted residual central distribution scheme [31, 24]. This explicit scheme provides third-order accuracy on hybrid meshes. Boundary conditions are handled with the Navier-Stokes Characteristics Boundary Condition (NSCBC) formulation [98, 91]. The Wall-Adapting Local Eddy-Viscosity (WALE) model [95] is used to compute the SGS viscosity. The parallel conduction solver is based on the same data structure as AVBP and uses an explicit scheme for time advancement. The dynamic code coupler PALM, initially developed for ocean-atmosphere coupling [67, 18], is used for the coupling strategy.

The test case is a cooled blade of the T120 cascade, which was designed by Rolls Royce Deutschland for the European project AITEB [52]. The experiments were conducted in the High-speed Cascade Wind Tunnel of the Institute of Jet Propulsion of Aachen [133, 56, 41]. The highly-loaded high-pressure turbine airfoil of the T120 cascade was designed to have a large separation on the pressure side. The blade is operated at a Reynolds number of $3.8 \times 10^5$ and a Mach number of 0.87, based on the exit velocity and the chord.

The film cooling device of the T120D blade is composed of three holes located on the pressure side, repeted in the spanwise direction to form a pattern of jet rows (see Fig. 3.4 for a single pattern). The first row of jets is placed near the stagnation point and has cylindrical holes with a compound angle against the main stream. The second jet comes from fan-shaped holes with zero compound angle located at approximately 20 % of the axial chord length. A third

row of cylindrical holes is placed at approximately 35 % of the axial chord. The temperature difference between the mainstream ($T_1^t = 333.15$ K) and cooling ($T_c^t = 303.15$ K) flows is limited to 30 K to facilitate measurements. The blade is made of plexiglass with a low conductivity of $0.184\ W \cdot \mathrm{m}^{-1} \cdot \mathrm{K}^{-1}$, which makes the CHT problem difficult to treat.

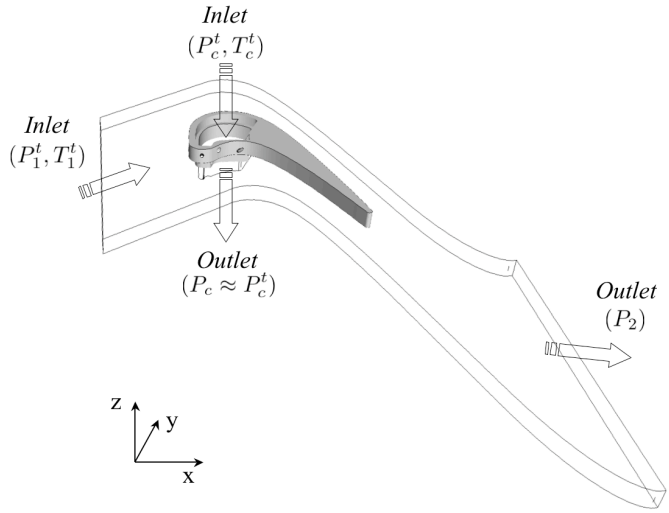


Figure 3.4: Fluid computational domain.

The computational domain covers one cooling hole pattern in the spanwise direction, with periodicity boundary conditions. This simplification neglects endwall effects but retains the three-dimensionality of the flow. Periodicity conditions are also applied on the azimuthal boundaries of the flow domain. The unstructured mesh is composed of 6.5 millions of tetrahedral elements for the fluid zone, and 600 000 elements within the solid. Specific care is devoted to the tetrahedral cell isotropy in the wall regions: the maximum values of grid spacings on the blade surface expressed in wall units are about $\Delta x^+ \approx \Delta y^+ \approx \Delta z^+ \approx 40$. In the dilution zone, grid spacings are smaller than 5 wall units. As shown in Fig. 3.4, the three film-cooling holes and the plenum used to inject the cooling air are also included in the fluid domain. The skin meshes are the same for the fluid and the solid so that no interpolation error is introduced at this level when CHT is simulated.

### 3.2.2 Adiabatic results

Adiabatic simulations with RANS and LES are first presented. The objective is to contrast the RANS and LES approaches and to provide a reference to assess the CHT computations reported in the next section. The RANS computation is performed with Fluent, using the $k - \omega/SST$ turbulence model [87].

Figure 3.5 depicts an instantaneous snapshot of vorticity (left) and a field of mixture fraction showing the path of cooling air in the main stream (right). The LES predicts an intense turbulence intensity and mixing in the region of the three jets. Downstream from the jets, the strong acceleration on the pressure side relaminarizes the flow and forces the cooling air against the blade surface. At the beginning of the suction side, the boundary layer is rather laminar. Then, the flow accelerates up to supersonic velocities. A weak shock appears at a reduced abscissa of about 0.75 (indicated by a dotted line in Fig. 3.5) and destabilizes the boundary layer. Vortex shedding develops behind the blade.

Figure 3.6 presents an instantaneous isosurface of temperature, illustrating the mixing of the cooling jet with the main flow. It shows that the first jet mixes rapidly with the hot gases.

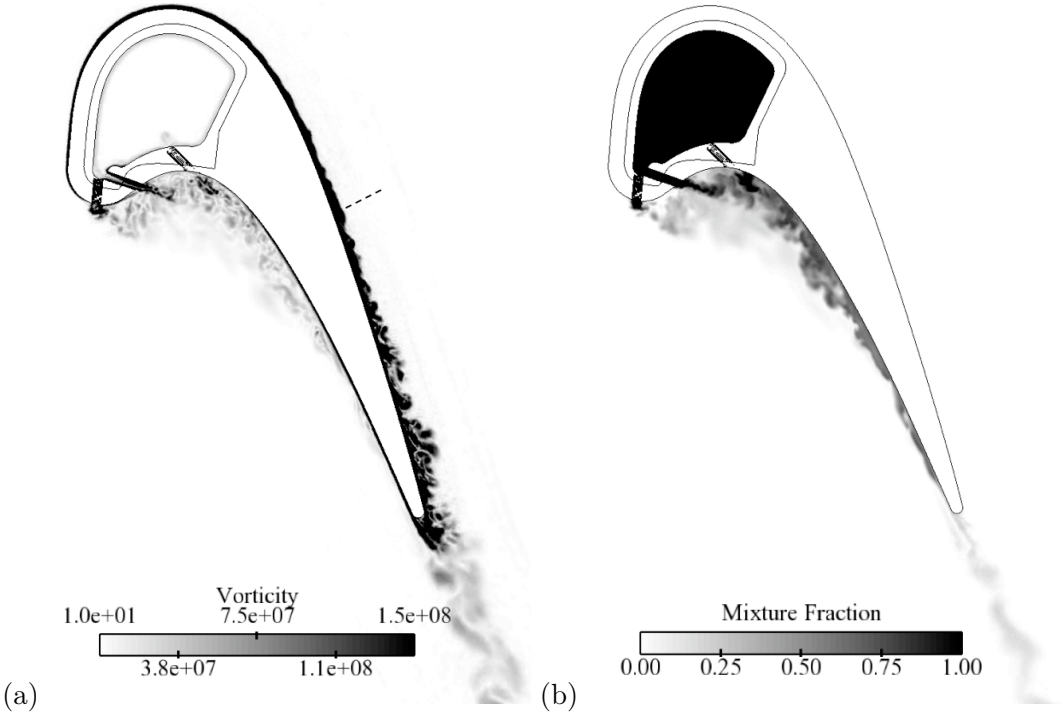


Figure 3.5: Instantaneous snapshot of (a) vorticity and (b) distribution of cooling air within a cutting plane at constant $z$ passing thought jet 2. The dashed line on (a) represents the approximate position of the shock at 75% of the axial chord.

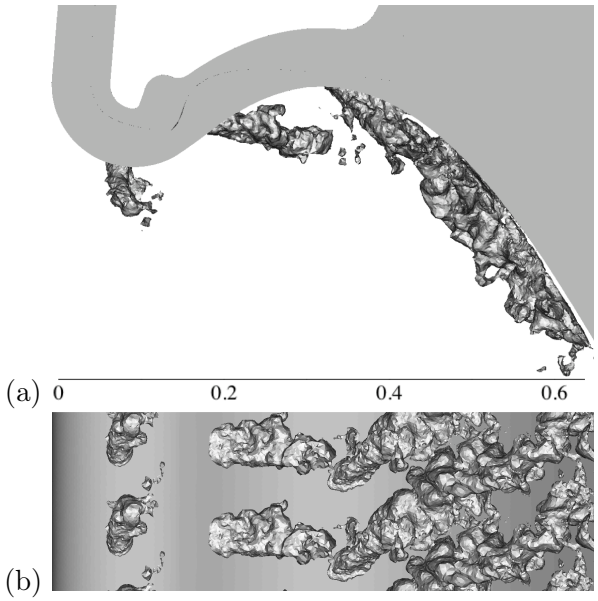


Figure 3.6: Instantaneous isosurface of temperature $T = 318\ K$: (a) $z$ view and (b) $y$ view.

Protected by the concave shape of the blade and by the first jet, the cooling air of the second hole penetrates more into the main flow, until it mixes with the third jet. Jet 3 is aligned with the primary flow and remains coherent until it impacts the blade in a region between reduced abscissa of 0.5 to 0.6.

The pressure distribution over the blade is then analyzed in terms of isentropic Mach number $M_{is}(\mathbf{x})$, defined Eq. (3.1). LES and experimental time-averaged distributions of $M_{is}(\mathbf{x})$ are compared in Fig. 3.7. Although the shock position on the suction side is not perfectly captured, the overall agreement between LES and experimental results is quite fair.

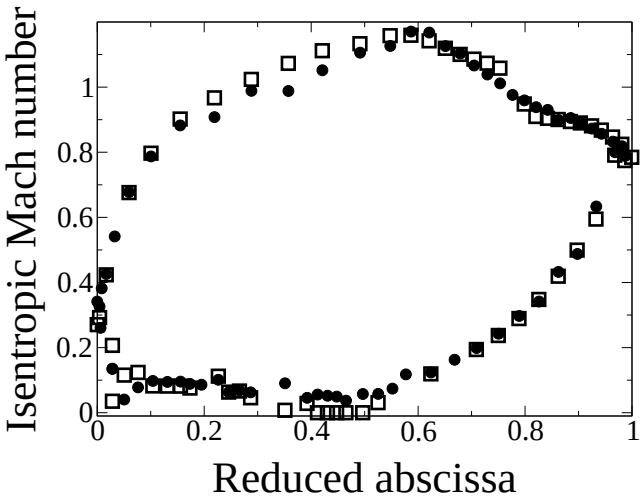


Figure 3.7: Time-averaged isentropic Mach number (Eq. 3.1) along the blade: •, adiabatic LES; □, experiment.

Wall temperatures $T_w^t(\mathbf{x})$ are presented in Fig. 3.8 in terms of cooling efficiency, defined as:

$$\Theta(\mathbf{x}) = \frac{T_1^t - T_w^t(\mathbf{x})}{T_1^t - T_c^t}, \tag{3.2}$$

where $T_1^t$ and $T_c^t$ are the total temperatures at the inlets of the mainstream and plenum, respectively. As expected, in the region of the jets (reduced abscissa up to 0.45) the cooling efficiencies obtained with the adiabatic simulations are lower than the experimental values: without heat transfer to the solid, the fluid temperature at the wall is too low. Downstream of the impact of the jets on the blade, the adiabatic LES fits the experimental level of $\Theta$, whereas the RANS computation over-estimates it. In the experiment, the film of colder air that forms after the interaction between the jets and the surface of the blade maintains the wall temperature close to adiabatic one. Hence, the LES captures fairly well the air mass flow through the jets as well as the mixing of the cooling air with the main stream. That is not the case for the RANS simulation. Indeed, even if the RANS computation reproduces the real air mass flow rates ejected by the holes, the simulation does not describe mixing correctly. As a result, the jets remain coherent on a too long distance without mixing with the hot stream and too much cold air impacts the blade surface, hence the overestimation of $\Theta$ close to the trailing edge.

Both LES and RANS simulations exhibit a non-physical peak of $\Theta$ near the trailing edge. This peak is due to an over-expansion near the trailing edge which does not appear in the experiment. The round trailing edge of the T120D blade profile and a lack of resolution in this region cause this difficulty in the computation, as already reported in the literature [27, 85].

This test case clearly shows that the LES approach gives better prediction of the cooling efficiency than the RANS one, both in terms of trends and absolute levels.

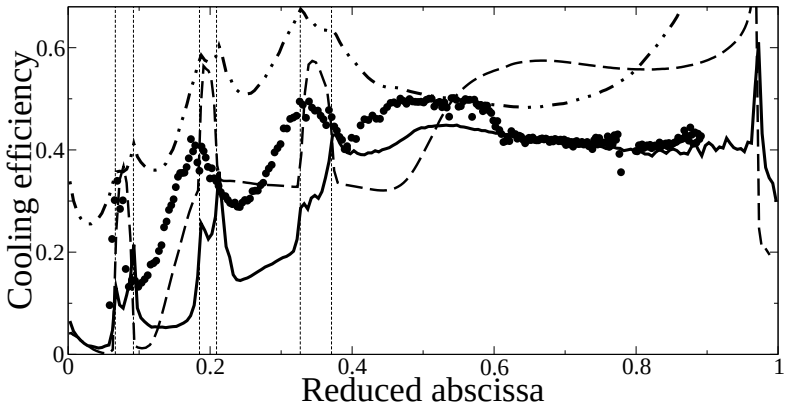


Figure 3.8: Time and spanwise averaged cooling efficiency (Eq. 3.2) versus abscissa on the pressure side as a function reduced abscissa: •, experiment from UNIBW; − adiabatic LES; −− adiabatic RANS; −··− coupled LES.

### 3.2.3 Coupled simulations

This sub-section presents a fully coupled simulation of the T120D blade obtained with a two-step methodology:

1. Initialization of the coupled calculation with:
   - a converged adiabatic fluid simulation (presented in the previous sub-section),
   - a converged solid computation with imposed boundary temperatures given by the adiabatic fluid solution.
2. Coupled simulation.

The converged state is obtained in 10 characteristic solid time scales $\tau_s$ and requires about 4800 CPU hours. At the converged state, the net heat flux through the blade reaches zero (*i.e.*, the mean temperature of the blade is stabilized at the value of the thermal boundary layer adiabatic (or friction) temperature). Results not shown in the present note indicate that the pressure distribution over the blade is not affected by the coupling, so the analysis focuses on thermal aspects.

Figure 3.8 shows measurements, adiabatic and coupled results of the cooling efficiency $\Theta(x)$ spanwise and time averaged along pressure side. As mentioned previously, the adiabatic temperature field (solid line) over-predicts the real one. The main contribution of conduction throughout the blade is to reduce the wall temperature on the pressure side and thus to increase $\Theta(x)$ (dot-dashed line). The global form of the reduced temperature from the coupled simulation matches the experimental trends better than for the adiabatic results. Differences in the absolute levels are explained by an insufficient wall resolution used the LES, and by the experimental difficulties and uncertainties for temperature measurements and processing (in particular spanwise averaging). The strong flow acceleration caused by the blade induces large thermal gradients not-well resolved by the simulation, which leads to an underestimation of the thermal fluxes as well as to non-physical values of cooling efficiency at the trailing edge.

Figure 3.9 compares experimental and numerical cooling efficiency fields on a 2D plot over the pressure side. The computation matches the experimental visualization fairly well. Figure 3.9 evidences the thermal effects of the cooling jets on the vane. Jet 1 is folded back against the surface by the main stream, but detaches rapidly and mixes with the hot gases due to the

curvature of the blade. Downstream of the second hole, a streak with higher efficiency and a spot with enhanced cooling close to the ejection location indicate a partially attached jet. A streak with a lower surface temperature is also visible downstream of the third jet. Jet 3 seems to be the most active in the cooling process: it protects the blade from the hot stream up to a reduced abscissa of 0.5. The curvature of the pressure side induces a slack film coverage: the concave shape of the surface spreads the cooling air laterally along the spanwise direction, as explained by Schwarz and Goldstein [120].

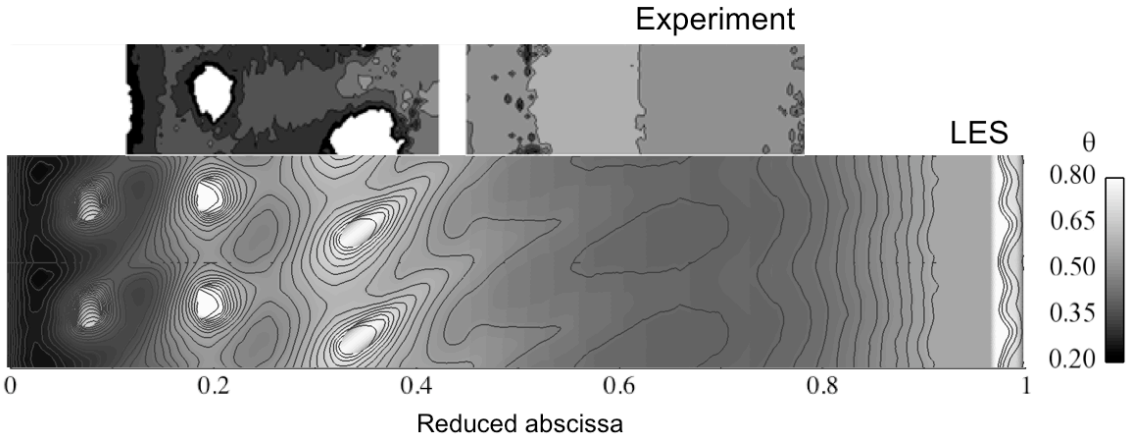


Figure 3.9: 2D plot of time-averaged cooling efficiency on the pressure side: comparison of experimental results and coupled simulation. The scale of $\Theta$ corresponds only to the LES field.

To sum up, this case demonstrates the better potential for LES to predict film cooling. As illustrated with the adiabatic results, the main reason for this is its ability to predict jet-in-crossflow turbulent mixing, which is well known to be a challenging features for RANS models. The coupling strategy presented improves the trend of the results, although some discrepancies with the experiment remain.

# Chapter 4

# Conclusion

Industrial turbomachinery flows are very complex, due to important viscous and three-dimensional effects [70], as well as complex turbulent mechanisms [69, 17]. Turbomachinery components design now heavily rely on the extensive use of CFD simulations to predict aerothermal performances [22, 57]. With the increase of computing power and the progresses of numerical methods on the one hand, and the need to design compact machines with large operating range on the other hand, 3D unsteady turbulent simulations are now more and more required in the design process [141, 42].

As turbulent effects become significant in the structuring of the mean flow, with strong anisotropy, laminar to turbulent transition, and natural instabilities such as vortex shedding, the limits of the (U)RANS framework tend to be approached.

In this context, the LES approach is a very effective way to handle complex turbulent features. However, there are still relatively few applications of this technique in the context of turbomachinery flows.

The objective of this lecture was to provide an overview of what have been accomplished in the published literature, and to illustrate it with two case studies. The overall goal was to give emphasis of what gain can be expected, and at what cost.

## Synthesis of the literature survey

The literature survey shows that most of the published tubomachinery-related applications deal with relatively simple or idealized configurations. Complex engineering applications still receive little attention, with very few publications dealing with fully 3D geometry, and even less with multistage machines.

From a quantitative point of view, it appears that LES brings accuracy gains that strongly depend on the applications and the flow feature observed: pressure and temperature profiles downstream an axial compressor close to the nominal operating point are only slightly better predicted [48], whereas heat fluxes can change dramatically in some cases (see Fig. 3.8 or Ref. [12]). For the turbine stator case presented in section 3.1, the Strouhal number characterizing the vortex shedding at the blade trailing edge is very significantly closer to the experimental value than the URANS result.

From a qualitative point of view, unsteady features are – of course – much more pronounced with the LES approach (see Fig 3.2 for instance), which can in turn affect the quantitative prediction [12]. When laminar–turbulent transition is involved, the gain is obvious [104].

## Future challenges and perspectives

Several challenges are still faced by LES in the turbomachinery context. In the authors' opinion, the followings are some of the most important.

First, as with any numerical simulation, there is the issue of the computational mesh. The literature survey indicate that most turbomachinery codes use structured meshes. With the ever increasing need to model complex geometries, sliding mesh and Chimera (overset grids) are a solution in the structured-grid approach. In the LES framework, higher-order interpolation schemes will be needed. The alternative is to resort to unstructured grids, but then the issue will be the development of high-order spatial discretization schemes (see further). In all cases, the mesh requirements close to the wall seem more stringent in the LES approach than with the RANS framework, and the question is raised of wether $\Delta y^+ \simeq 1$ is sufficient.

A second issue, obviously related to the previous one, is the need for high-order spatial discretization schemes for the convective fluxes. It is the authors' opinion that schemes classically used for turbomachinery simulations, such as the Jameson [59] and Roe [109] schemes, will not be sufficient. These schemes suffer from a too high level of dissipation that is not suited for the LES approach. This is, of course, to be balanced with the grid resolution. An alternative already in use is the AUSM+ scheme [77], which can be third-order accurate when the limiter is suppressed (which is not suitable when dealing with shocks). Perspectives are to be found with schemes such as the WENO class (see Ref. [126] for instance), the RBC scheme [75] in an implicit time-integration framework, and the compact schemes developed by Lele [74] for finite differences or Lacor *et al.* [66] for finite volumes.

Another issue is the treatment of the boundary conditions. Local one-dimensional non reflecting boundaries, which are very often used for turbomachinery flows computations, may not be sufficient for the LES framework, unless very large grid cells are used close to the border to damp perturbations (with obvious impact on the accuracy). The boundary conditions developed by Tam [134] are good candidate in this respect.

Finally, the literature survey has showed that computing rotor/stator interactions is probably one of the main challenges faced by the LES approach in the turbomachinery field. As a matter of fact, all of the published rotor/stator studies either modify the geometry to get periodic boundary conditions [108, 102] or compute the full annulus [63]. Given the significant step in mesh resolution from (U)RANS to LES (Tab. 3.1), it is much likely that phase-lag (chorochronic) boundary conditions for LES will be needed to make possible industrial single-passage LES rotor/stator computations. However, it will then be necessary to transfer through the interface the most part of the large frequency range of turbulence captured by LES, which contrasts with the current practice.

To conclude with a more practical word, there is still a need for detailed comparisons of (U)RANS and LES approaches, particularly in terms of CPU costs (see Tab. 3.1 for an example of such a comparison). From the physical standpoint, comparisons of RANS and LES results for turbomachinery applications must continue, in order to get a more comprehensive perspective of what can be achieved with both methods. To sum up, gains and costs, as well as best-practice guidelines, still need thorough assessment for LES to be used as an industrial design tool for turbomachines.

# Bibliography


[1] S. Acharya, M. Tyagi, and A. Hoda. Flow and heat transfer predictions for film cooling. *Heat transfer in gas turbine systems. Annals of the New York Academy of Sciences*, 934:110–125, 2001.

[2] H. I. Andersson and M. Lygren. LES of open rotor–stator flow. *International Journal of Heat and Fluid Flow*, 27(4):551–557, 2006.

[3] A. Arnone and R. Pacciani. Rotor-stator interaction analysis using the Navier–Stokes equations and a multigrid method. *Journal of Turbomachinery*, 118(4):679–689, 1996.

[4] T. Arts. Calculation of the Three-Dimensional, Steady, Inviscid Flow in a Transonic Axial Turbine Stage. *Journal of Engineering for Gas Turbine and Power*, 107:286–292, 1985.

[5] T. Arts, M. Lambert de Rouvroit, and A. W. Rutherford. Aero-thermal investigation of a highly loaded transonic linear turbine guide vane cascade – a test case for inviscid and viscous flow computations. Technical Report 174, VKI, 1990.

[6] A. Azzi and D. Lakehal. Perspectives in modeling film cooling of turbines blades by transcending conventional two-equation turbulence models. *Journal of Turbomachinery*, 124:472–484, 2002.

[7] E. Balaras, C. Benocci, and I. Piomelli. Two-layer approximate boundary conditions for large-eddy simulations. *AIAA Journal*, 34:1111–1119, 1996.

[8] M. Baragon, H. Bijl, and M. van Tooren. Bubble bursting and laminar separation unsteadiness on a multi-element high lift configuration. *Applied Scientific Research*, 71(1-4):279–296, 2003.

[9] J. Bardina, J. Ferziger, and W. Reynolds. Improved turbulence models based on large-eddy simulation of homogeneous, incompressible turbulent flows. Technical Report TF 19, Stanford University, 1983.

[10] J. Bardina, J. Ferziger, and R. Rogallo. Effect of rotation on isotropic turbulence: computation and modeling. *Journal of Fluid Mechanics*, 154:321–336, 1985.

[11] P. Batten, P. Spalart, and M. Terracol. Use of Hybrid RANS–LES for Acoustic Source Predictions. In C. Wagner, T. Huttl, and P. Sagaut, editors, *Large-Eddy Simulation for Acoustics*. Cambridge University Press, 2007.

[12] D. L. Black, K. V. Meredith, and C. E. Smith. LES simulations predicting heat transfer and wall temperature on turbine inlet guide vanes at high fuel-air ratios. In *Proc. of ISABE*, number 1201, 2005.

[13] M. Boileau, G. Staffelbach, B. Cuenot, T. Poinsot, and C. Berat. LES of an Ignition Sequence in a Full Helicopter Combustor. *Combustion and Flame*, 154:2–22, 2008.

[14] J. P. Boris, F. F. Grinstein, E. S. Oran, and R. Kolbe. New insights into large eddy simulation. *Fluid Dynamics Research*, 10:199–228, 1992.

[15] J. Boudet, J. Caro, L. Shao, and E. Lévêque. Numerical studies towards practical large-eddy simulation. *Journal of Thermal Science*, 16(4):328–336, 2007.

[16] G. Boudier, L. Y. M. Gicquel, T. Poinsot, D. Bissières, and C. Bérat. Comparison of LES, RANS and experiments in an aeronautical gas turbine combustion chamber. *Proc. Combust. Inst.*, 31:3075–3082, 2007.

[17] P. Bradshaw. Turbulence modeling with application to turbomachinery. *Progress in Aerospace Science*, 32:575–624, 1996.

[18] S. Buis, A. Piacentini, and D. Déclat. Palm: A computational framework for assembling high performance computing applications. *Concurrency and Computation*, 18(2):231–245, 2005.

[19] R. S. Bunker. Gas turbine heat transfer: Ten remaining hot gas path challenges. *Journal of Turbomachinery*, 129:193–201, 2007.

[20] R. K. Byskov, C. B. Jacobsen, and N. Pedersen. Flow in a centrifugal pump impeller at design and off-design conditions—part ii: Large eddy simulations. *Journal of Fluids Engineering*, 125(1):73–83, 2003.

[21] L. Cambier and J. Veuillot. Status of the elsA Software for Flow Simulation and Multi-Disciplinary Applications. In *46th AIAA Aerospace Sciences Meeting and Exhibit*, Reno, Nevada, Jan. 2008. AIAA-2008-0664.

[22] M. Casey. The industrial use of CFD in the design of turbomachinery. *AGARD-LS-195*, 1994.

[23] M. Casey, P. Dalbert, and P. Roth. On the use of viscous flow calculations in the design and analysis of industrial centrifugal compressors. *ASME Paper*, (90-GT-2), 1990.

[24] O. Colin and M. Rudgyard. Development of high-order taylor-galerkin schemes for unsteady calculations. *Journal of Computational Physics* , 162(2):338–371, 2000.

[25] T. Coton, T. Arts, M. Lefebvre, and N. Liamis. Unsteady and calming effects investigation on a very high-lift LP turbine blade—part i: Experimental analysis. *Journal of Turbomachinery*, 125(2):281–290, 2003.

[26] S. Deck. Zonal Detached Eddy Simulation of the Flow Around a High-Lift Configuration. *AIAA Journal*, 43(11):2372–2384, 2005.

[27] J. Denton and W. N. Dawes. Computational fluid dynamics for turbomachinery design. In M. E. Publications, editor, *Proceedings of the Institution of Mechanical Engineers. Part C, Journal of mechanical engineering science*, volume 213, pages 107–124, London, United Kingdom, 1999.

[28] J. D. Denton. An Improved Time-Marching Method for Turbomachinery Flow Calculation. *ASME Journal of Engineering for Power*, 105:514–524, 1983.

[29] J. D. Denton. The 1993 IGTI Scholar Lecture: Loss Mechanisms in Turbomachines. *Journal of Turbomachinery*, 115(4):621–656, 1993.

[30] J. D. Denton and U. K. Singh. Time Marching Methods for Turbomachinery Flow Calculation. In E. Schmidt, editor, *Application of Numerical Methods to Flow Calculations in Turbomachines*, VKI Lecture Series. Von Kármán Institute for Fluid Dynamics, Rhode-St-Genèse (Belgique), 1979.

[31] J. Donea and A. Huerta. *Finite Element Methods for Flow Problems*. John Wiley & Sons Inc, New York, 2003.

[32] D. Drikakis and W. Rider. *High-Resolution Methods for Incompressible and Low-Speed Flows*. Springer-Verlag, Berlin, 2005.

[33] F. Duchaine, A. Corpron, L. Pons, V. Moureau, F. Nicoud, and T. Poinsot. Development and assessment of a coupled strategy for conjugate heat transfer with large eddy simulation. Application to a cooled turbine blade. *International Journal of Heat and Fluid Flow*, In press, 2009.

[34] F. Duchaine, S. Mendez, F. Nicoud, A. Corpron, V. Moureau, and T. Poinsot. Conjugate heat transfer with large eddy simulation for gas turbine components. *Comptes Rendus de l'Académie des Sciences – Mécanique*, In press, 2009.

[35] G. Dufour, J.-B. Cazalbou, X. Carbonneau, and P. Chassaing. Assessing rotation/curvature corrections to eddy-viscosity models in the calculations of centrifugal-compressor flows. *Journal of Fluids Engineering*, 130(9):091401, 2008.

[36] M. G. Dunn. Convective heat transfer and aerodynamics in axial flow turbines. *Journal of Turbomachinery*, 123:637–686, 2001.

[37] S. J. Eastwood, P. G. Tucker, H. Xia, and C. Klostermeier. Developing Large Eddy Simulation for Turbomachinery Applications. *Philosophical Transactions of the Royal Society A*, 367(1899):2999–3013, 2009.

[38] M. A. Elyyan and D. K. Tafti. Large eddy simulation investigation of flow and heat transfer in a channel with dimples and protrusions. *Journal of Turbomachinery*, 130(4):041016, 2008.

[39] P. Ferrand, J. Boudet, J. Caro, S. Aubert, and C. Rambeau. Analyses of URANS and LES Capabilities to Predict Vortex Shedding for Rods and Turbines. In K. C. Hall, R. E. Kielb, and J. P. Thomas, editors, *Unsteady Aerodynamics, Aeroacoustics and Aeroelasticity of Turbomachines*. Springer, 2006.

[40] M. Germano, U. Piomelli, P. Moin, and W. H. Cabot. A dynamic subgrid-scale eddy viscosity model. *Physics of Fluids A: Fluid Dynamics*, 3(7):1760–1765, 1991.

[41] R. A. Gomes and R. Niehuis. Film cooling effectiveness measurements with periodic unsteady inflow on highly loaded blades with main flow separation. In *Proceedings of ASME Turbo Expo 2009: Power for Sea, Land and Air*, Orlando, Florida, USA, June 2009.

[42] N. Gourdain and F. Lebœuf. Unsteady simulation of an axial compressor stage with casing and blade passive treatments. *Journal of Turbomachinery*, 131(2):021013, 2009.

[43] N. Gourdain, F. Lebœuf, and H. Miton. Numerical simulation of rotating stall in a subsonic compressor. In *Proc. of the 40th AIAA/ASME/SAE/ASEE Joint Propulsion Conference and Exhibit*, number AIAA-2004-3929, 2006.

[44] N. Gourdain, X. Ottavy, and A. Vouillarmet. Experimental and numerical investigation of unsteady flows in a high speed three stages compressor. In *European Turbo-machinery Conference*, Graz, Austria, Mar. 2009.

[45] G. Grotzbach. *Direct and large eddy simulation of turbulent channel flows*, pages 1337–1391. Gulf Publ., New Jersey, 1987.

[46] W. Haase, M. Braza, and A. Revell, editors. *DESider – A European Effort on Hybrid RANS–LES modelling*. Springer, 2009.

[47] C. Hah. Navier-Stoles Analysis of Three-Dimensional Unsteady Flows Inside Turbine Stages. In *AIAA Paper*, number 92-3211, 1992.

[48] C. Hah. Large eddy simulation of transonic flow field in NASA rotor 37. In *Proc. of the 47th Aerospace Sciences Meeting*, number 1061, 2009.

[49] C. Hah, J. Bergner, and H. SCHIFFER. Short length-scale rotating stall inception in a transonic axial compressor – criteria and mechanisms. In *Proc. of GT2006 ASME Turbo Expo 2006: Power for Land, Sea and Air*, number GT2006-90045, 2006.

[50] C. Hah, M. Voges, M. Mueller, and H. P. Schiffer. Investigation of Unsteady Flow Behavior in Transonic Compressor Rotors with LES and PIV. In *Proc. of ISABE*, number 2009-02, 2009.

[51] C. A. Hah. Navier-Stokes Analysis of Three-Dimensional Turbulent Flow Inside Turbine Blade Rows at Design and Off-Design Conditions. *ASME J. Eng. Gas Turbines Power*, 106:421–429, 1984.

[52] F. Haselbach and P. Schiffer. Aiteb - an european research project on aero-thermodynamics of turbine endwalls and blades. *International Journal of Thermal Science* , 13(2):97–108, 2007.

[53] Y.-H. Ho and B. Lakshminarayana. Computation of Unsteady Viscous Flow Through Turbomachinery Blade Row Due to Upstream Rotor Wakes. *Journal of Turbomachinery*, 117(4):541–552, 1995.

[54] A. Hoda and S. Acharya. Predictions of a Film Coolant Jet in Crossflow With Different Turbulence Models. *Journal of Turbomachinery*, 122(3):558–569, 2000.

[55] H. Hodson. Turbulence modelling for unsteady flows in axial turbine: Turmunsflat. Technical Report Final TR CT96-1043, Brite-Euram Project, von Karman Institute, 2000.

[56] L. Homeier and F. Haselbach. Film cooling of highly loaded blades. In *XVIII International Symposium on Air Breathing Engines (ISABE)*, number AIAA-2005-1114, Munich, Germany, September 2005.

[57] J. H. Horlock and J. D. Denton. A Review of Some Early Design Practice Using Computational Fluid Dynamics and a Current Perspective. *Journal of Turbomachinery*, 127(1):5–13, 2005.

[58] I. V. Iourokina and S. K. Lele. Towards Large Eddy Simulation of Film-Cooling Flows on a Model Turbine Blade Leading Edge. In *Proc of the 43rd Aerospace Sciences Meeting and Exhibit, Reno, NV*, number AIAA Paper 2005-0670, 2005.

[59] A. Jameson, W. Schmidt, and E. Turkel. Numerical Solutions of the Euler Equations by Finite Volume Methods Using Runge-Kutta Time-Stepping Schemes. In *AIAA 14th Fluid and Plasma Dynamic Conference*, number AIAA Paper 81-1259, Palo Alto, June 1981.

[60] J. Jeong and F. Hussain. On the Identification of a Vortex. *Journal of Fluid Mechanics*, 285:69–94, 1995.

[61] J. Jouhaud, L. Y. M. Gicquel, B. Enaux, and M. Esteve. Large-Eddy-Simulation Modeling for Aerothermal Predictions Behind a Jet in Crossflow. *AIAA Journal*, 45(10):2438–2447, 2007.

[62] C. Kato, M. Kaiho, and A. Manabe. An Overset Finite-Element Large-Eddy Simulation Method With Applications to Turbomachinery and Aeroacoustics: Flow Simulation and Modeling. *Journal of Applied Mechanics*, 70(1):32–43, 2003.

[63] C. Kato, H. Mukai, and A. Manabe. Large-Eddy Simulation of Unsteady Flow in a Mixed-Flow Pump. *International Journal of Rotating Machinery*, 9(5):345–351, 2003.

[64] C. Kato, Y. Yamade, H. Wang, Y. Guo, M. Miyazawa, T. Takaishi, S. Yoshimura, and Y. Takano. Numerical Prediction of Sound Generated from Flows with a Low Mach Number. *Computers and Fluids*, 36(1):53–68, 2007.

[65] M. Klein, A. Sadiki, and J. Janicka. A digital filter based generation of inflow data for spatially developing direct numerical or large eddy simulations. *Journal of Computational Physics*, 186(2):652–665, 2003.

[66] C. Lacor, S. Smirnov, and M. Baelmans. A finite volume formulation of compact central schemes on arbitrary structured grids. *Journal of Computational Physics*, 198(2):535–566, 2004.

[67] T. Lagarde, A. Piacentini, and O. Thual. A new representation of data-assimilation methods: The palm flow-charting approach. *Q. J. R. Meteorol. Soc.*, 127(571):189–207, 2001.

[68] D. Lakehal, G. S. Theodoridis, and W. Rodi. Computation of Film Cooling of a Flat Plate by Lateral Injection from a Row of Holes. *International Journal of Heat and Fluid Flow*, 19(5):418–430, 1998.

[69] B. Lakshminarayana. Turbulence modeling for complex shear flows. *AIAA Journal*, 24(12):1900–1917, 1986.

[70] B. Lakshminarayana. *Fluid Dynamics and Heat Transfer of Turbomachinery*. John Wiley & Sons, Inc., New York, NY, USA, 1996.

[71] S. Lardeau and M. Leschziner. Unsteady RANS Modeling of Wake-Induced Transition in Linear LP-Turbine Cascades. *AIAA Journal*, 44(8):1845—1865, 2006.

[72] S. Lee, H.-J. Kim, and A. Runchal. Large Eddy Simulation of Unsteady Flows in Turbomachinery. *Proceedings of the Institution of Mechanical Engineers*, 218, 2004.

[73] A. H. Lefebvre. *Gas Turbines Combustion*. Taylor & Francis, 1999.

[74] S. K. Lele. Compact Finite Difference Schemes with Spectral-like Resolution. *Journal of Computational Physics*, 103(1):16–42, 1992.

[75] A. Lerat and C. Corre. A Residual-Based Compact Scheme for the Compressible Navier-Stokes Equations. *Journal of Computational Physics*, 170:642–675, July 2001.

[76] D. K. Lilly. A proposed modification of the Germano subgrid-scale closure method. *Physics of Fluids A: Fluid Dynamics*, 4(3):633–635, 1992.

[77] M.-S. Liou. A sequel to AUSM: AUSM+. *Journal of Computational Physics*, 129(2):364–382, 1996.

[78] D. Lohmann. Prediction of ducted radiation fan aeroacoustics with a lifting surface method. Technical Report DGLR/AIAA92-02-098, DLR, 1992.

[79] T. S. Lund, X. Wu, and K. D. Squires. Generation of turbulent inflow data for spatially-developing boundary layer simulations. *Journal of Computational Physics*, 140:233–258, Mar. 1998.

[80] M. Lygren and H. I. Andersson. Turbulent flow between a rotating and a stationary disk. *Journal of Fluid Mechanics*, 426(-1):297–326, 2001.

[81] K. Mahesh, G. Constantinescu, and P. Moin. A numerical method for large-eddy simulation in complex geometries. *Journal of Computational Physics*, 197(1):215–240, 2004.

[82] M. Manna, M. Mulas, and G. Cicatelli. Vortex Shedding Behind a Blunt Trailing Edge Turbine Blade. *Int. J. Turbo Jet Engines*, 14:145–157, 1997.

[83] I. Mary and P. Sagaut. Large-eddy simulation of flow around an airfoil near stall. *AIAA Journal*, 40(6), 2002.

[84] G. Medic and P. A. Durbin. Toward Improved Film Cooling Prediction. *Journal of Turbomachinery*, 124(2):193–199, 2002.

[85] Y. Mei and A. Guha. Implicit numerical simulation of transonic flow through turbine cascades on unstructured grids. In P. E. Publishing, editor, *Proceedings of the Institution of Mechanical Engineers. Part A. Journal of power and energy*, volume 219, pages 95–47, Bury St Edmunds, United Kingdom, 2005.

[86] S. Mendez and F. Nicoud. Large-eddy simulation of a bi-periodic turbulent flow with effusion. *Journal of Fluid Mechanics* , 598:27–65, 2008.

[87] F. R. Menter. Zonal two equation k-w turbulence models for aerodynamic flows. In *Fluid Dynamics, Plasmadynamics, and Lasers Conference, 23rd*, number AIAA-1993-2906, Orlando, FL, USA, July 1993.

[88] V. Michelassi, J. G. Wissink, J. Frölich, and W. Rodi. Large-eddy simulation of flow around low-pressure turbine blades with incoming wakes. *AIAA Journal*, 41(11):2143–2156, 2003.

[89] R. Mittal, S. Venkatasubramanian, and F. M. Najjar. Large-eddy simulation of flow through a low-pressure turbine cascade. In *Proc. of the 15th Computational Fluid Dynamics Conference*, number AIAA Paper 2001-2560, 2001.

[90] S. Moreau, M. Roger, and J. Christophe. Flow features and self-noise of airfoils near stall or in stall. In *Proc. of the 15th AIAA/CEAS Aeroacoustics Conference (30th AIAA Aeroacoustics Conference)*, number AIAA Paper 2009-3196, 2009.

[91] V. Moureau, G. Lartigue, Y. Sommerer, C. Angelberger, O. Colin, and T. Poinsot. Numerical methods for unsteady compressible multi-component reacting flows on fixed and moving grids. *Journal of Computational Physics* , 202(2):710–736, 2005.

[92] F. Muldoon and S. Acharya. Direct numerical simulation of a film cooling jet. In *Proc. of the 2004 TurboExpo*, number ASME Paper GT2004-41685. ASME, 2004.

[93] C. Muthanna and W. J. Devenport. Wake of a compressor cascade with tip gap, part 1: Mean flow and turbulence structure. *AIAA Journal*, 42(11):2320–2331, 2004.

[94] C. Muthanna and W. J. Devenport. Wake of a compressor cascade with tip gap, part 2: Effects of endwall motion. *AIAA Journal*, 42(11):2332–2340, 2004.

[95] F. Nicoud and F. Ducros. Subgrid-scale stress modelling based on the square of the velocity gradient. *Flow, Turbulence and Combustion*, 62(3):183–200, 1999.

[96] M. M. Opoka and H. P. Hodson. Transition on the T106 LP turbine blade in the presence of moving upstream wakes and downstream potential fields. *Journal of Turbomachinery*, 130(4):041017, 2008.

[97] M. M. Opoka, R. L. Thomas, and H. P. Hodson. Boundary layer transition on the high lift T106A low-pressure turbine blade with an oscillating downstream pressure field. *Journal of Turbomachinery*, 130(2):021009, 2008.

[98] T. Poinsot and D. Veynante. *Theoretical and Numerical Combustion.* R.T. Edwards, 2nd edition., 2005.

[99] C. Prière, L. Y. M. Gicquel, P. Kaufmann, W. Krebs, and T. Poinso. Large eddy simulation predictions of mixing enhancement for jets in cross-flows. *Journal of Turbulence*, 5(5):1468–5248, 2004.

[100] M. M. Rai. Navier-Stokes Simulations of Rotor/Stator Interactions Using Patched and Overlaid Grids. *Journal of Propulsion and Power*, 3:387–396, 1987.

[101] M. M. Rai. A Direct Numerical Simulation of Transition and Turbulence in a Turbine. In *AIAA, 47th Aerospace Sciences Meeting, Reno*, number AIAA Paper 2009-0584, 2009.

[102] M. M. Rai. A Direct Numerical Simulation of Turbine Rotor–Stator Interaction. In *39th AIAA Fluid Dynamics Conference, San Antonio, Texas*, number AIAA Paper 2009-3685, 2009.

[103] A. Randriamampianina and S. Poncet. Turbulence characteristics of the bödewadt layer in a large enclosed rotor-stator system. *Physics of Fluids*, 18(5):055104, 2006.

[104] B. Ravedy, I. Mary, P. Sagaut, and N. Liamis. High-resolution large-eddy simulation of flow around low-pressure turbine blade. *AIAA Journal*, 41(3):390–397, 2003.

[105] G. Reboul, C. Polacsek, S. Lewy, and S. Heib. Aeroacoustic computation of ducted-fan broadband noise using LES data. In *Proc. of the Acoustics'08 Conference*, 2008.

[106] G. Reboul, C. Polacsek, S. Lewy, and S. Heib. Ducted-fan broadband noise simulations using unsteady or averaged data. In *Proc. of the Inter-Noise 2008 Conference*, 2008.

[107] S. Richard, O. Colin, O. Vermorel, A. Benkenida, C. Angelberger, and D. Veynante. Towards Large Eddy Simulation of Combustion in Spark Ignition Engines. *Proc. Combust. Inst.*, 31:3059–3066, 2006.

[108] J. Riou, S. Lewy, and S. Heib. Large eddy simulation for predicting rotor-stator broadband interaction fan noise. In *Proc. of the Inter-Noise 2007 Conference*, 2007.

[109] P. L. Roe. Approximate Riemann Solvers, Parameter Vectors and Difference Schemes. *Journal of Computational Physics*, 43, 1981. pp. 357-372.

[110] A. Roux, L. Y. M. Gicquel, Y. Sommerer, and T. J. Poinsot. Large eddy simulation of mean and oscillating flow in a side-dump ramjet combustor. *Journal of Combustion and Flame* , 152(1-2):154–176, 2008.

[111] A. Rozati and D. K. Tafti. Large eddy simulation of leading edge film cooling–part ii: Heat transfer and effect of blowing ratio. *Journal of Turbomachinery*, 130:041015–1–041015–7, 2008.

[112] Y. Rozenberg, M. Roger, and S. Moreau. Fan Blade Trailing-Edge Noise Prediction Using RANS Simulations. In *Proc. of the Acoustics'08 Conference*, 2008.

[113] P. Sagaut and S. Deck. Large-Eddy Simulation for Aerodynamics: Status and Perspectives. *Philosophical Transactions of the Royal Society A*, 367:2849–2860, 2009.

[114] A. K. Saha and S. Acharya. Flow and heat transfer in an internally ribbed duct with rotation: An assessment of large eddy simulations and unsteady reynolds-averaged navier-stokes simulations. *Journal of Turbomachinery*, 127(2):306–320, 2005.

[115] S. Sarkar. The Effect of Passing Wakes on a Separating Boundary Layer Along a Low-Pressure Turbine Blade Through Large-Eddy Simulation. *Proc. Inst. Mech. Eng., Part A*, 221:551–564, 2007.

[116] S. Sarkar. Influence of Wake Structure on Unsteady Flow in a Low Pressure Turbine Blade Passage. *Journal of Turbomachinery*, 131(4):221–231, 2009.

[117] S. Sarkar and P. R. Voke. Large-eddy simulation of unsteady surface presure over a low-pressure turbine blade due to interactions of passing wakes and inflexional boundary layer. *Journal of Turbomachinery*, 128:221–231, 2006.

[118] R. Schiele and S. Wittig. Gas turbine heat transfer: Past and future challenges. *Journal of Propulsion and Power* , 16(4):583–589, July 2000.

[119] T. Schönfeld and T. Poinsot. Influence of boundary conditions in LES of premixed combustion instabilities. In *Annual Research Briefs* , pages 73–84. Center for Turbulence Research, NASA Ames/Stanford Univ., 1999.

[120] S. G. Schwarz and R. J. Goldstein. The two-dimensional behavior of film cooling jets on concave surfaces. *Journal of Turbomachinery*, 111:124–130, 1989.

[121] E. Serre, E. C. D. Arco, and P. Bontoux. Annular and spiral patterns in flows between rotating and stationary discs. *Journal of Fluid Mechanics*, 434(-1):65–100, 2001.

[122] E. Séverac, S. Poncet, E. Serre, and M.-P. Chauve. Large eddy simulation and measurements of turbulent enclosed rotor-stator flows. *Physics of Fluids*, 19(8):085113, 2007.

[123] E. Séverac and E. Serre. A spectral vanishing viscosity for the LES of turbulent flows within rotating cavities. *Journal of Computational Physics*, 226(2):1234–1255, 2007.

[124] E. A. Sewall and D. K. Tafti. Large eddy simulation of flow and heat transfer in the 180-deg bend region of a stationary gas turbine blade ribbed internal cooling duct. *Journal of Turbomachinery*, 128(4):763–771, 2006.

[125] E. A. Sewall and D. K. Tafti. Large eddy simulation of flow and heat transfer in the developing flow region of a rotating gas turbine blade internal cooling duct with coriolis and buoyancy forces. *Journal of Turbomachinery*, 130(1):011005, 2008.

[126] C. W. Shu. High-order Finite Difference and Finite Volume WENO Schemes and Discontinuous Galerkin Methods for CFD. *International Journal of Computational Fluid Dynamics*, 17(2):107–118, 2003.

[127] M. L. Shur, P. R. Spalart, M. K. Strelets, and A. K. Travin. Towards the prediction of noise from jet engines. *International Journal of Heat and Fluid Flow*, 24(4):551–561, 2003.

[128] C. H. Sieverding, H. Richard, and J.-M. Desse. Turbine blade trailing edge flow characteristics at high subsonic outlet mach number. *Journal of Turbomachinery*, 125(2):298–309, 2003.

[129] P. E. Smirnov and F. R. Menter. Sensitization of the SST Turbulence Model to Rotation and Curvature by Applying the Spalart–Shur Correction Term. *Journal of Turbomachinery*, 131(4):041010, 2009.

[130] D. L. Sondak and D. J. Dorney. Simulation of Vortex Shedding in a Turbine Stage. *Journal of Turbomachinery*, 121(3):428–435, 1999.

[131] P. Spalart, W. Jou, M. Strelets, and S. Allmaras. Comments on the Feasibility of LES for Wings and on a Hybrid RANS/LES Approach. In C. Liu and Z. Liu, editors, *Advances in DNS/LES*. Greyden Press, 1997.

[132] P. Stadtmuller and L. Fottner. A test case for the numerical investigation of wake passing effects of a highly loaded LP turbine cascade blade. In *Proc. of the ASME Turbo Expo*, number ASME Paper 2001-GT-311, 2001.

[133] W. Sturm and L. Fottner. The high-speed cascade wind-tunnel of the german armed forces university munich. In *8th Symposium on Measuring Techniques for Transonic and Supersonic Flows in Cascades and Turbomachines*, Genova, Italy, October 1985.

[134] C. K. W. Tam and Z. Dong. Wall boundary conditions for high-order finite-difference schemes in computational aeroacoustics. *Theoretical and Computational Fluid Dynamics*, 6(5-6):303–322, 1994.

[135] L. Tang. RANS Simulation of Low-Reynolds-Number Airfoil Aerodynamics. In *44th AIAA Aerospace Sciences Meeting and Exhibit 9 - 12 January 2006, Reno, Nevada*, number AIAA Paper 2006-249, 2006.

[136] N. Tauveron. Simulation of a compressor cascade with stalled flow using large eddy simulation with two-layer approximate boundary conditions. *Nuclear Engineering and Design*, Article in press, 2008.

[137] A. Travin, M. Shur, M. Strelets, and P. Spalart. Detached-Eddy Simulations Past a Circular Cylinder. *Flow, Turbulence and Combustion*, 63(1-4):293–313, 1999.

[138] P. G. Tucker and S. Lardeau. Applied Large Eddy Simulation. *Philosophical Transactions of the Royal Society A*, 367(1899):2809–2818, 2009.

[139] M. Tyagi and S. Acharya. Large eddy simulation of film cooling flow from an inclined cylindrical jet. *Journal of Turbomachinery*, 125(4):734–742, 2003.

[140] M. Tyagi and S. Acharya. Large eddy simulation of turbulent flows in complex and moving rigid geometries using the immersed boundary method. *International Journal for Numerical Methods in Fluids*, 48(7):691–722, 2005.

[141] E. van der Weide, G. Kalitzin, J. U. Schluter, and J. J. Alonso. Unsteady Turbomachinery Computations Using Massively Parallel Platforms. In *44th AIAA Aerospace Sciences Meeting and Exhibit, Reno, USA*, 2006.

[142] M. Wang and P. Moin. Computation of Trailing-Edge Flow and Noise Using Large-Eddy Simulation. *AIAA Journal*, 38(12):2201–2209, 2000.

[143] D. C. Wilcox. Reassessment of the scale-determining equation for advanced turbulence models. *AIAA Journal*, 26(11):1299–1310, 1988.

[144] J. Windte, U. Scholz, and R. Radespiel. Validation of the RANS-simulation of laminar separation bubbles on airfoils. *Aerospace science and technology*, 10(6):484–494, 2006.

[145] X. Wu and P. A. Durbin. Evidence of longitudinal vortices evolved from distorted wakes in a turbine passage. *Journal of Fluid Mechanics*, 446(-1):199–228, 2001.

[146] X. Wu and K. D. Squires. Prediction and investigation of the turbulent flow over a rotating disk. *Journal of Fluid Mechanics*, 418(-1):231–264, 2000.

[147] D. You, R. Mittal, M. Wang, and P. Moin. Large-eddy simulation of a rotor tip-clearance flow. In *Proc. of the 40th Aerospace Science Meeting and Exhibit*, number AIAA Paper 2002-0981, 2002.

[148] D. You, R. Mittal, M. Wang, and P. Moin. Computational methodology for large-eddy simulation of tip-clearance flows. *AIAA Journal*, 42(2):271–279, Feb. 2004.

[149] D. You, M. Wang, R. Mittal, and P. Moin. Study of rotor tip-clearance flow using large eddy simulation. In *Proc. of the 41st Aerospace Science Meeting and Exhibit*, number AIAA Paper 2003-0838, 2003.

[150] D. You, M. Wang, P. Moin, and R. Mittal. Effects of tip-gap size on the tip-leakage flow in a turbomachinery cascade. *Physics of Fluids*, 18(10):105102, 2006.